Transmembrane insertases and *N*-glycosylation critically determine synthesis, trafficking, and activity of the nonselective cation channel TRPC6

Received for publication, March 4, 2019, and in revised form, June 28, 2019 Published, Papers in Press, July 2, 2019, DOI 10.1074/jbc.RA119.008299

Brianna E. Talbot[‡], David H. Vandorpe[‡], Brian R. Stotter[‡§], Seth L. Alper[‡], and Johannes S. Schlondorff[‡1]

From the [‡]Division of Nephrology, Beth Israel Deaconess Medical Center, Harvard Medical School, Boston, Massachusetts 02215 and the [§]Division of Nephrology, Boston Children's Hospital, Harvard Medical School, Boston, Massachusetts 02115

Edited by Mike Shipston

Transient receptor potential cation channel subfamily C member 6 (TRPC6) is a widely expressed ion channel. Gain–of–function mutations in the human TRPC6 channel cause autosomal-dominant focal segmental glomerulosclerosis, but the molecular components involved in disease development remain unclear. Here, we found that overexpression of gain–of–function TRPC6 channel variants is cytotoxic in cultured cells. Exploiting this phenotype in a genome-wide CRISPR/Cas screen for genes whose inactivation rescues cells from TRPC6-associated cytotoxicity, we identified several proteins essential for TRPC6 protein expression, including the endoplasmic reticulum (ER) membrane protein complex transmembrane insertase. We also identified transmembrane protein 208 (TMEM208), a putative component of a signal recognition particle-independent (SND) ER protein-targeting pathway, as being necessary for expression of TRPC6 and several other ion channels and transporters. TRPC6 expression was also diminished by loss of the previously uncharacterized WD repeat domain 83 opposite strand (WDR83OS), which interacted with both TRPC6 and TMEM208. Additionally enriched among the screen hits were genes involved in *N*-linked protein glycosylation. Deletion of the mannosyl (α-1,3-)-glycoprotein β-1,2-*N*-acetylglucosaminyltransferase (MGAT1), necessary for the generation of complex *N*-linked glycans, abrogated TRPC6 gain–of–function variant-mediated Ca^{2+} influx and extracellular signal-regulated kinase activation in HEK cells, but failed to diminish cytotoxicity in cultured podocytes. However, mutating the two TRPC6 *N*-glycosylation sites abrogated the cytotoxicity of mutant TRPC6 and reduced its surface expression. These results expand the targets of TMEM208-mediated ER translocation to include multipass transmembrane proteins and suggest that TRPC6 *N*-glycosylation plays multiple roles in modulating channel trafficking and activity.

TRPC6 is one of seven members of the canonical transient receptor potential (TRPC)[2] subfamily of TRP channels (1, 2). TRPC6 functions as a tetrameric nonselective cation channel (3) and assembles either as a homomer or as a heteromer with TRPC1, -C3, or -C7 (4–6). Activation and regulation of TRPC6 channel activity are complex and remain incompletely understood (7). TRPC6 is directly activated by diacylglycerol (3) and augmented by 20-hydroxyeicosatetraenoic acid (8–10). It is best characterized acting downstream of $G\alpha_q$-coupled receptors (11, 12), but it is also activated downstream of tyrosine kinases (13–15) and by reactive oxygen species (14, 16–19). The ability of membrane deformation to activate TRPC6, directly (20) or indirectly (21), remains controversial (22) and may be cell type–specific (9, 23–29). TRPC6 directly or indirectly mediates increases in intracellular calcium concentration (30–33), leading to activation of signaling pathways (34) that includes calcineurin–NFAT (35–37), CREB (38–40), ERK (38), RhoA (41–43), and calpain-mediated proteolysis (44).

TRPC6 has a broad tissue- and cell-type expression profile, including smooth muscle cells, epithelial cells, endothelial cells, and immune cells (45, 46). TRPC6 functions in animal and *in vitro* models (34), including differentiation, activation, and proliferation of myofibroblasts (47, 48); modulation of organ fibrosis (48–50); promotion of pathologic cardiac hypertrophy (35, 36) and pulmonary edema (51); modulation of glomerular diseases, including diabetic nephropathy (52–56); promotion of neuronal survival and dendritic outgrowth (57, 58); and regulation of leukocyte migration (59, 60).

Human TRPC6 gene mutations are a cause of autosomal-dominant focal segmental glomerulosclerosis (FSGS), a progressive glomerular kidney disease (61, 62). Disease mutations are located within the cytoplasmic amino- or carboxyl-tails of the channel, predominantly in the ankyrin repeats and the

This work was supported by National Institutes of Health Grants R01DK115438 (to J. S.) and T32 DK007726 (B. R. S.). The authors declare that they have no conflicts of interest with the contents of this article. The content is solely the responsibility of the authors and does not necessarily represent the official views of the National Institutes of Health.
This article contains Table S1.

[1] To whom correspondence should be addressed. Tel.: 617-667-0508; Fax: 617-667-0495; E-mail: jschlond@bidmc.harvard.edu.

[2] The abbreviations used are: TRPC, transient receptor potential channel; TRP, transient receptor potential; CRISPR, clustered regularly interspaced short palindromic repeats, ER, endoplasmic reticulum; EMC, ER membrane protein complex; ERAD, endoplasmic reticulum-associated protein degradation; FSGS; focal segmental glomerulosclerosis; GOF, gain–of–function; MTT, 3-(4,5-dimethylthiazol-2-yl)-2,5-diphenyltetrazolium bromide; NTC, no target control; RFP, red fluorescent protein; sgRNA, single-guide RNA; SRP, signal recognition particle; SND, SRP-independent; STRING, String Tool for the Retrieval of Interacting Genes/Proteins; Tricine, *N*-[2-hydroxy-1,1-bis(hydroxymethyl)ethyl]glycine; Tet, tetracycline; HBSS, Hanks' buffered saline solution; ANOVA, analysis of variance; EndoH, endoglycosidase H; PNGaseF, peptide:*N*-glycosidase F; NFAT, nuclear factor of activated T-cell; ERK, extracellular signal-regulated kinase.

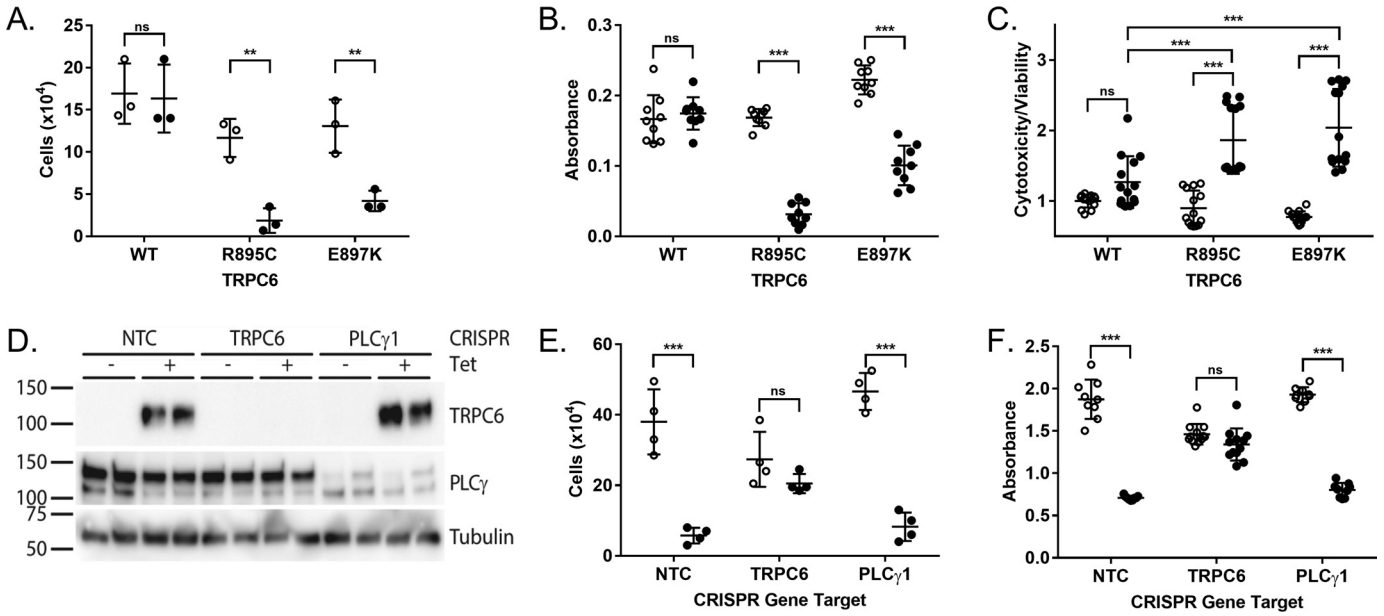

Figure 1. TRPC6 gain–of–function mutations are cytotoxic. *A–C,* equal numbers of TRex293 cells expressing the indicated tetracycline-inducible FLAG–TRPC6 construct were grown in the absence (*open circles*) or presence (*solid circles*) of tetracycline. *A,* cells were trypsinized and counted after 90 h of growth. *B,* colorimetric MTT assay was performed to compare metabolic activity after growth for 72 h. *C,* relative cytotoxicity/viability ratio of the indicated TRPC6-expressing cells after 24 h of induction. *D–F,* tetracycline-inducible TRPC6 R895C-expressing cells were transfected with LentiCRISPR constructs encoding sgRNAs either with no target (NTC) or targeting TRPC6 or PLCγ1; two different sgRNA sequences were tested for each target. FLAG–TRPC6 expression was induced with tetracycline as indicated. *D,* expression of TRPC6, PLCγ1, and tubulin was assayed by Western blotting. Cell count (*E*) and MTT assay (*F*) were performed after 72 h of tetracycline induction. Shown are means ± S.D. and individual values. Statistical analysis was performed using two-way ANOVA with Tukey's multiple comparisons test (*C*) or multiple *t*-testing using the Holm-Sidak method; **, $p < 0.01$; ***, $p < 0.001$; *ns*, $p > 0.05$.

coiled-coil sequences. Most mutations are reported to increase TRPC6-mediated current amplitude, delay channel inactivation, and/or increase intracellular calcium levels (61–65). Other studies have reported disease-associated mutations impairing channel activity, at least in response to certain stimuli (64, 66). Why TRPC6 mutations cause a renal-limited disease in humans despite the channel's many reported functions in model systems remains unclear.

We do not yet know how the various disease-associated TRPC6 mutations cause a gain–of–function (GOF) phenotype. It has been suggested that mutations alter cell-surface expression (15, 61), although we (67) and others (68) have not found this to be the case. Cryo-EM structures demonstrate clustering of disease mutations at the interface between the ankyrin repeats and the C-terminal coiled coil (69, 70). This structure has prompted the hypothesis that the mutations alter allosteric gating, but confirmatory data are lacking. Although basal currents of TRPC6 GOF mutants are not of higher magnitude than those of the WT channel (67), they do lead to increased calcineurin-NFAT (67) and ERK (71) signaling in the absence of exogenous stimuli. We have hypothesized that some yet unidentified endogenous intermittent signal activates TRPC6 in this setting.

To better understand potential regulators of mutant TRPC6 and its downstream effects, we exploited the cytotoxic phenotype of cells overexpressing TRPC6 GOF mutants to perform a genome-wide CRISPR-Cas screen to identify genes whose inactivation rescued cells from cytotoxicity. The ER membrane protein complex (EMC), TMEM208 (recently identified as the mammalian homolog of SND2 (72)), and WDR83OS were revealed as necessary for effective expression of TRPC6 protein. Multiple enzymes involved in protein glycosylation were also identified as necessary for activity of TRPC6 GOF mutants. Loss of complex *N*-glycans on proteins due to *MGAT1* deletion abolished TRPC6-mediated calcium influx without altering channel surface expression, whereas deletion of TRPC6 *N*-glycosylation sites diminished surface expression. In summary, TRPC6 expression requires the activities of two transmembrane insertases, whereas complex *N*-glycosylation of TRPC6 is required for TRPC6 channel function but not for its surface expression.

Results

CRISPR/Cas screen utilizing the cytotoxicity of TRPC6 GOF mutants for selection

We considered that overexpression of TRPC6 with GOF mutations is detrimental to cellular survival or proliferation in light of unsuccessful attempts at generating stable cell lines constitutively expressing these mutant TRPC6 forms. Utilizing previously generated stable cell lines with inducible expression of WT or the FSGS mutant TRPC6 (67, 71), we found enhanced cytotoxicity and impaired proliferation upon overexpression of the GOF mutant, but not WT, TRPC6, as measured by cell count (Fig. 1*A*), MTT assay (Fig. 1*B*), and a cell viability/cytotoxicity assay (Fig. 1*C*). Furthermore, we have been unable to maintain cultured podocytes transduced to express GOF TRPC6 mutants (data not shown), consistent with published data reporting enhanced podocyte apoptosis upon overexpression of GOF TRPC6 (73). CRISPR-Cas–mediated knockout of TRPC6, but not PLCγ1 knockout or use of a no-target control (NTC) single-guide RNA (sgRNA), abrogated the cytotoxic

effect of tetracycline induction (Fig. 1, *D–F*), suggesting that the cytotoxicity of GOF TRPC6 could be used in a positive selection CRISPR screen for genes that regulate TRPC6 function or toxicity.

We used a pooled library of lentivirus-encoded CRISPR-Cas sgRNAs (74) to identify genes necessary for the loss of cell viability induced by overexpression of the TRPC6 E897K GOF mutant (Table S1). Three of the four sgRNAs targeting TRPC6 were enriched; the nonenriched sgRNA targets TRPC6 at a splice site and is thus not predicted to target the cDNA construct driving TRPC6 GOF expression in our system. The top 63 gene hits identified in our screen using single-guide RNA set enrichment analysis were entered into STRING (Search Tool for the Retrieval of Interacting Genes/Proteins; www.string-db.org). This generated a network (Fig. 2*A*) significantly enriched for protein–protein interactions (enrichment *p* value: $<1.0 \times 10^{-16}$). Gene ontology process and component analysis identified enrichment of genes involved in *N*-linked glycosylation and in the ubiquitin-dependent endoplasmic reticulum-associated protein degradation (ERAD) pathway (75, 76) and genes found in the nuclear outer membrane–endoplasmic reticulum membrane network and EMC (Fig. 2*B*). NCLN (nicalin), NOMO, and TMEM147, reported components of the nodal modulator complex (77), as well as NOMO2 and NOMO3 were also among the screen hits. In validation experiments, we tested two sgRNA sequences, distinct from those in the Brunello library (Table 1), for each of 12 screen hits for their ability to rescue cell viability upon induction of the TRPC6 R895C GOF mutant. These genes were chosen to represent various protein complexes or processes (EMC and ERAD pathways, *N*-linked glycosylation, the nodal modulator complex), or because their potential mechanisms of action were unclear or of potential biological interest. A majority of these sgRNAs significantly enhanced cell viability following induction of TRPC6 R895C, as compared with a nontarget control sgRNA (Fig. 2*C*).

To investigate the potential mechanism whereby knockout of these genes rescued cell viability, we examined TRPC6 protein levels (Fig. 2*D*). Guide RNAs targeting EMC2, EMC6, CCDC47, and TMEM208 substantially decreased TRPC6 protein levels. None of the tested sgRNAs significantly altered tetracycline induction of TRPC6 mRNA levels (Fig. 2*E*). The ability of the two WDR83OS sgRNAs to rescue cell viability correlated with their effect on reducing TRPC6 protein levels; testing several additional sgRNAs confirmed the association between loss of WDR83OS expression and decreased TRPC6 protein levels (Fig. 2*F*). However, we were unable to rescue TRPC6 expression by transfection of a WDR83OS expression construct (Fig. 2*G*), leaving in question this gene's status as a true modulator of TRPC6 expression. In contrast, the expression of a CRISPR-resistant TMEM208 construct rescued TRPC6 R895C expression in TMEM208 knockout cells (Fig. 2*H*), further validating TMEM208 as a modulator of TRPC6 protein levels. MGAT1 knockout significantly altered TRPC6 mobility on SDS-PAGE (Fig. 2*D*), consistent with the role of MGAT1 in generating hybrid and complex *N*-glycans (78).

EMC and TMEM208 are each required for expression of multiple transmembrane proteins, but not for each other's expression

The EMC is a 10-protein complex in mammalian cells (79) that functions as a transmembrane domain insertase, necessary for membrane insertion of tail-anchored proteins with moderately hydrophobic transmembrane domains (80) and for expression of various polytopic membrane proteins (81). In contrast, little is known about the function of TMEM208; it has been localized to the ER and implicated in regulation of autophagy and ER stress (82). We therefore explored the potential role of TMEM208 in modulating TRPC6 protein levels, and whether TMEM208 might be tied to EMC function. Expression of FLAG–TRPC6 is diminished in EMC2, EMC6, and TMEM208 knockout cells (Fig. 3*A*). EMC2 and EMC6 proteins are each mutually dependent upon the expression of the other (Fig. 3*A*), consistent with previous reports that knockout of one component of the EMC complex reduces expression of the entire complex (80). However, neither EMC component is affected by loss of TMEM208 nor is TMEM208 dependent upon expression of EMC2 or EMC6, suggesting that TMEM208 functions independently of the EMC. Expression of WDR83OS was not appreciably altered in any of the cell lines.

The expression of several additional transmembrane proteins was assessed in EMC- and TMEM208-deficient cells to address the possible requirement for TMEM208 and EMC genes for TRPC6 expression specifically or for transmembrane protein expression in general (Fig. 3, *B* and *C*). Expression plasmids encoding FLAG-tagged potassium channel KCNN4/IK1 (Fig. 3*B*) and HA-tagged K-Cl cotransporter SLC12A4/KCC1 (Fig. 3*C*) were co-transfected with TRPC6 expression constructs into control (NTC) CRISPR-treated cells or EMC2, EMC6, or TMEM208 knockout cells. Cytoplasmic red fluorescent protein (RFP) expression plasmid was included as a control for transfection efficiency (Fig. 3*B*). Multimembrane-spanning proteins KCNN4 and SLC12A4 showed comparably poor expression in cells lacking either the EMC component or TMEM208. In contrast, levels of the endogenous ER resident protein calnexin, a type 1 single transmembrane span protein, were not appreciably affected by loss of the EMC or of TMEM208. In sum, these results suggest that the EMC and TMEM208 are required for expression of diverse polytopic transmembrane proteins, including TRPC6.

TRPC6 interacts with TMEM208 and WDR83OS

WDR83OS is a 106-amino acid predicted transmembrane protein of unknown function. Overexpressed, epitope-tagged TRPC6 and WDR83OS could be co-immunoprecipitated and did not affect each other's expression levels (Fig. 4*A*). WDR83OS lacking its C-terminal 27 amino acids, including a predicted transmembrane domain, was expressed at lower levels than full-length protein, but it maintained its ability to immunoprecipitate TRPC6 (Fig. 4*B*). Interestingly, both WDR83OS constructs appear to preferentially interact with the lower molecular weight form of TRPC6, representing the immaturely *N*-glycosylated channel. A FLAG-tagged

WDR83OS construct lacking amino acids 1–37 failed to produce detectable protein (data not shown).

FLAG-tagged TMEM208 was also capable of immunoprecipitating HA–TRPC6 when co-expressed (Fig. 4*C*). Truncated forms of TMEM208 lacking either the C-terminal 69 amino acids (including the predicted third transmembrane domain) or the N-terminal 68 amino acids (including the predicted first two transmembrane domains) were still able to co-immunoprecipitate HA–TRPC6. However, compared with full-length TMEM208, the truncated mutants did not rescue TRPC6

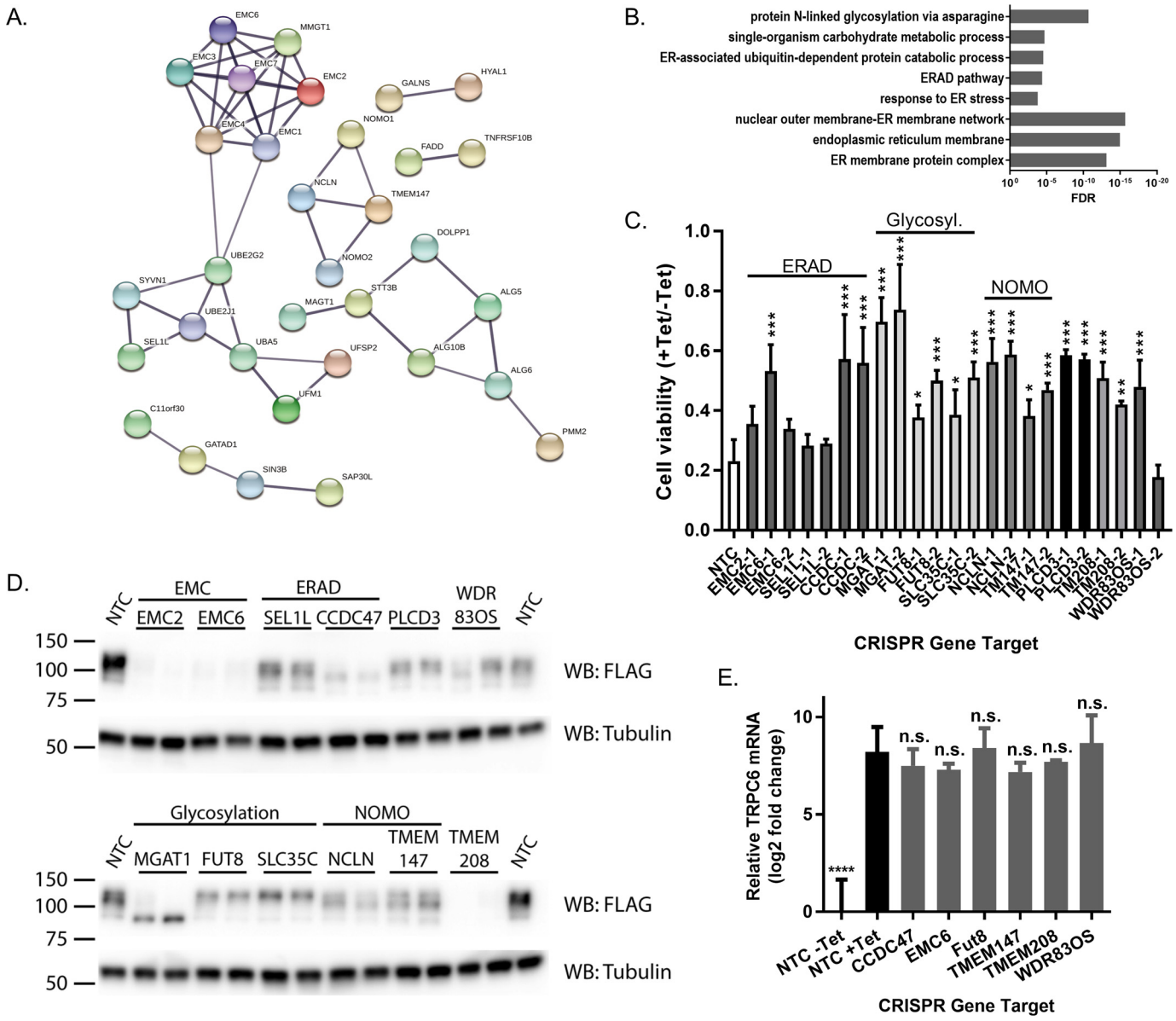

Table 1
CRISPR sgRNA sequences utilized in validation experiments

Gene target	sgRNA sequence
CCDC47_1	TCAGTGATTATGACCCGTTG
CCDC47_2	CATACCACTTGATCACTCAC
EMC2_1	CACAGAGTCAAGCGATTAAC
EMC2_2	ATACTCATTCAGCTCCCGAA
EMC6_1	ACGGCCGCCTCGCTGATGAA
EMC6_2	GACCTCGGTGTCAGCGCTGT
FUT8_1	ACGCGTACTCTTCCTATAGC
FUT8_2	TACTACCTCAGTCAGACAGA
MAN2B1_1	AGGTGCACGTTCAGCATGTT
MAN2B1_2	GCCTCACACACATGATGACG
MGAT1_1	GATTTCCTCGCCCGCGTCTA
MGAT1_2	CCGCGGGGAAGCGAAACTGC
NCLN_1	CCGTGCCCCAGGACGTCGTC
NCLN_2	CATGCAGCAGTACGACCTGC
PLCD3_1	CCTTGTGCCACGTGCGCGAG
PLCD3_2	GCAAGATCCGCTCGCGCACG
SEL1L_1	CAAACATCTCTCTCGCTGCC
SEL1L_2	AGCATATCGGTATCTCCAAA
SLC35C1_1	TGCCGATGAAGACCACCGAC
SLC35C1_2	GCTAGCCAGCACGCCGAAGA
TMEM147_1	GGTCCGAGTACAACGCCTTC
TMEM147_2	CTTGTCATGTCCCGGAATGC
TMEM208_1	TGGCCCCCAGTATGATCCGC
TMEM208_2	CTACCACTCTATGAGCTCGA
WDR83OS_1	GTCCGGCGTCGGGTCGTCCA
WDR83OS_2	TGGGTCCGACATATTGTTAG
WDR83OS_3	CCCGCCGAGCGAATGTAACC
WDR83OS_4	ACAATATGTCGGACCCACGG
WDR83OS_5	GTCCTCCGAGCTCCGAGAGT
WDR83OS_6	CCTAGCTGAAGTGGTGTGCT

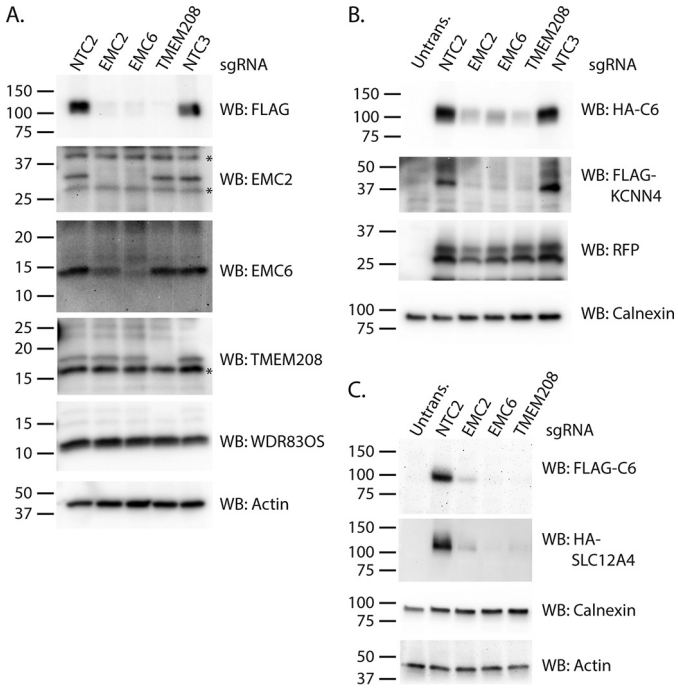

Figure 3. EMC and TMEM208 are necessary for expression of a variety of multipass transmembrane proteins. *A,* FLAG–TRPC6 R895C expression was induced by tetracycline in cells with CRISPR-mediated knockout of EMC2, EMC6, or TMEM208 or expressing control sgRNA (NTC). Western blot (*WB*) analysis demonstrates that FLAG–TRPC6 expression depends upon each of these three genes (*top panel*). In contrast, EMC2 and EMC6 expression are dependent on each other, but not on TMEM208, whereas TMEM208 protein levels are not altered by loss of either EMC component. Levels of endogenous WDR83OS were not appreciably different in these cell lines. *Asterisks* mark nonspecific bands. *B,* cells with CRISPR-mediated knockout of the genes indicated at the *top* of the panel were co-transfected with expression constructs for HA-tagged WT TRPC6, FLAG-tagged KCNN4, and RFP. Expression of the indicated proteins was then analyzed by Western blotting equal amounts of cell lysates. RFP was used as a control for transfection efficiency. *C,* the same CRISPR-modified cells as in *B* were co-transfected with expression constructs for FLAG–TRPC6 and HA-tagged SLC12A4/KCC1, lysed, and analyzed by Western blotting using the indicated antibodies. Endogenous calnexin was examined as a model single-pass type 1 transmembrane protein; actin served as a loading control.

expression as effectively when re-introduced into TMEM208 knockout cells (Fig. 4*D*).

Interestingly, in addition to TRPC6, we detected endogenous WDR83OS in the FLAG–TMEM208 immunoprecipitates (Fig. 4*C*). To ensure that this interaction was not dependent upon the presence of overexpressed TRPC6, we repeated the experiments in the absence of overexpressed TRPC6 (Fig. 4*E*), with similar results. V5-tagged TMEM208 was also immunoprecipitated by full-length and carboxyl-truncated FLAG–WDR83OS (Fig. 4*F*). However, TMEM208 knockout did not affect WDR83OS protein levels (Fig. 3*A*, 4*G*) nor did WDR83OS knockout alter TMEM208 levels (Fig. 4*G*). Immunofluorescence microscopy demonstrated partial co-localization of overexpressed TRPC6, TMEM208, and WDR83OS in perinuclear and reticular patterns, intracellular structures suggestive of ER (Fig. 4, *H–J*), providing evidence that these proteins have the opportunity to interact *in vivo*. Together, these results suggest that WDR83OS is a predominantly ER-localized protein capable of interacting with both TRPC6 and TMEM208.

Figure 2. CRISPR screen identifies genes necessary for TRPC6 GOF cytotoxicity. *A,* protein–protein interaction network generated by STRING analysis utilizing the top 63 gene hits identified in the CRISPR screen. Only genes demonstrating at least one high-confidence interaction with another hit are displayed. *B,* false discovery rate (*FDR*) for cellular processes and components most overrepresented among the top CRISPR hits, as defined by gene ontology. *C–E,* tetracycline-inducible TRPC6 R895C-expressing cells were transfected with LentiCRISPR constructs encoding either no target control sgRNAs (NTC) or sgRNAs targeting the indicated genes identified in the screen. Two independent sgRNAs were tested per gene. Antibiotic-selected cells were grown in the absence or presence of tetracycline to induce FLAG–TRPC6 R895C expression. *C,* relative cell viability, calculated as the ratio of live cells cultured in the presence *versus* absence of tetracycline for 96 h. *Bar shading groups* genes found in a complex or involved in a particular biological process. One-way ANOVA analysis with Dunnett's multiple comparisons test compared with NTC; *, $p < 0.05$; **, $p < 0.01$; ***, $p < 0.001$. *D,* Western blot analysis of FLAG–TRPC6 R895C expression after tetracycline induction in the indicated CRISPR cell lines. Tubulin served as a loading control. *E,* qPCR analysis of glyceraldehyde-3-phosphate dehydrogenase–normalized TRPC6 RNA expression after tetracycline induction in the indicated CRISPR cell lines, as compared with NTC cells grown in the absence or presence of tetracycline. One-way ANOVA analysis with Dunnett's multiple comparisons test compared with NTC with tetracycline; ****, $p < 0.0001$; *n.s.*, not significant. *F,* Western blot (*WB*) analysis of FLAG–TRPC6 R895C, WDR83OS, and actin in cells transfected with control NTC CRISPR construct or four distinct WDR83OS targeting CRISPR constructs. Loss of FLAG–TRPC6 expression correlated with the degree of WDR83OS knockout achieved. *G,* tetracycline-inducible TRPC6 R895C-expressing cells transfected with LentiCRISPR constructs encoding sgRNAs with either no target (NTC) or targeting two distinct sequences in WDR83OS (WDR83OS 1 and 4) were transfected with empty vector (*EV*) or plasmid encoding CRISPR-resistant HA-tagged WDR83OS as indicated. Cell lysates were subject to immunoblotting after treatment without or with tetracycline (+*Tet*) as indicated. Transfection of HA-WDR83OS plasmid produced WDR83OS protein levels higher than endogenous levels seen in NTC cell lines, but failed to significantly alter FLAG–TRPC6 protein levels. *H,* control NTC CRISPR (*TMEM KO* −) or TMEM208 CRISPR knockout (*TMEM KO* +) TRPC6 R895C inducible cells were transfected with plasmid encoding a CRISPR-resistant V5-tagged TMEM208 construct (+) or empty vector (−) as indicated, followed by tetracycline-induction of TRPC6 expression. Cell lysates were analyzed by Western blotting for expression of FLAG–TRPC6, TMEM208, and β-actin. V5-tagged TMEM208 (*open arrowhead*) runs as a slightly higher band than endogenous TMEM208 (*solid arrowhead*). The *asterisk* marks a nonspecific band.

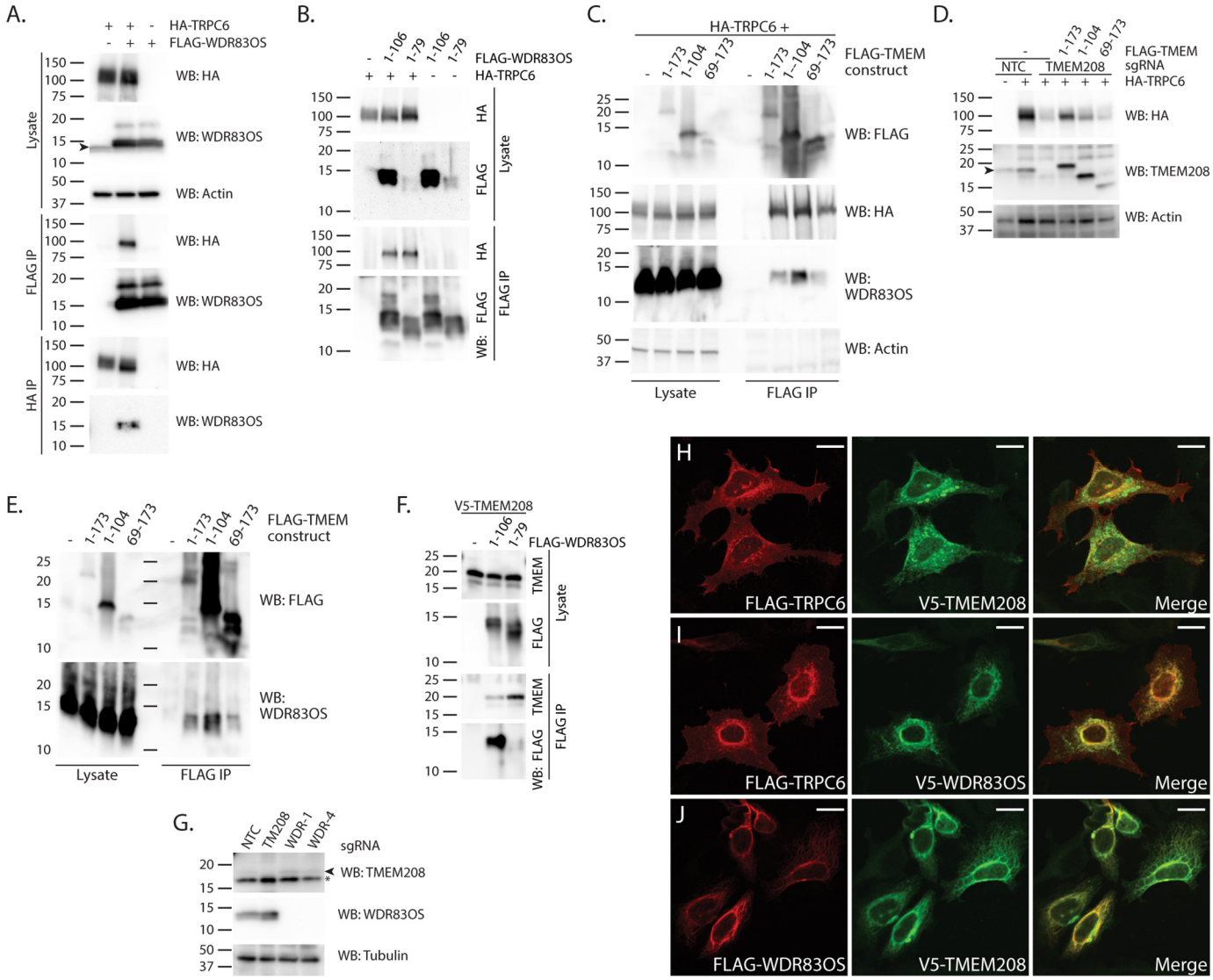

Figure 4. TRPC6, WDR83OS, and TMEM208 interact with each other. *A,* HEK 293T cells were transfected with HA-tagged WT TRPC6 and FLAG-tagged WDR83OS as indicated, lysed, and subjected to immunoprecipitation with anti-FLAG or anti-HA antibody. Whole lysates, and the FLAG and HA immunoprecipitates (*IP*), were probed with antibody against HA, WDR83OS, and β-actin as indicated. The *arrowhead* marks endogenous WDR83OS. *B,* cells were transfected with HA-tagged TRPC6 and either full-length (1–106) or C-terminal truncated (1–79) FLAG-tagged WDR83OS as shown. Cell lysates and anti-FLAG immunoprecipitates were analyzed by SDS-PAGE followed by Western blotting (*WB*) with HA or FLAG antibody as indicated. *C,* HEK cells were transfected with HA–TRPC6 and empty vector (−) or various FLAG-tagged TMEM208 constructs, including full-length TMEM208 (1–173), a C-terminal truncated construct (1–104), and an N-terminal truncated form (69–173). Cell lysates and FLAG immunoprecipitation samples were subject to SDS-PAGE and Western blotting with the indicated antibodies. Endogenous WDR83OS was detected in lysates and FLAG–TMEM208 immunoprecipitates. *D,* HEK cells were transfected with LentiCRISPR v2 plasmids encoding control (NTC) or TMEM208-targeting sgRNA as indicated (sgRNA). These cells were then transfected with plasmids encoding HA–TRPC6 and various FLAG–TMEM208 constructs as in *C*, lysed and analyzed by SDS-PAGE followed by Western blotting with the indicated antibodies. Co-expression of full-length (1–173) FLAG–TMEM208 rescued TRPC6 expression in the TMEM208 knockout cells to a greater extent than did the carboxyl- (1–104) or amino-terminal (69–173) truncated FLAG–TMEM208 constructs. The *arrowhead* in the *middle panel* marks endogenous TMEM208 present in control (NTC) CRISPR cells. *E,* lysates and FLAG immunoprecipitated material from HEK cells transfected with the indicated FLAG–TMEM208 expression constructs were subjected to SDS-PAGE and Western blotting with anti-FLAG and anti-WDR83OS antibodies as indicated. Endogenous WDR83OS was detected in all FLAG–TMEM containing immunoprecipitates, but not in immunoprecipitates from cells transfected with empty vector (−). *F,* V5–TMEM208 was transfected into HEK cells with control vector (−), full-length (1–106) FLAG–WDR83OS, or C-terminal truncated (1–79) FLAG–WDR83OS. Lysates and FLAG IP material were analyzed by Western blotting with antibodies against the FLAG-epitope or TMEM208 (*TMEM*) as indicated. *G,* HEK cells were transfected with LentiCRISPR v2 plasmids encoding sgRNAs without a target (NTC), targeting TMEM208 (*TMEM*), or targeting two different sequences of WDR83OS (*WDR-1* and *WDR-4*). Cell lysates were subjected to SDS-PAGE and Western blotting using the indicated antibodies. TMEM208 is highlighted by an *arrowhead*; the *asterisk* marks a nonspecific band. Tubulin served as a loading control. *H–J,* immunofluorescence microscopy of HeLa cells transiently transfected with FLAG–TRPC6 and V5-TMEM208 (*H*), FLAG–TRPC6 and V5-WDR83OS (*I*), and FLAG–WDR83OS and V5-TMEM208 (*J*). Individual channels are shown on the *left* and *middle panels*; the composite image is shown on the *right* (*merge*). *Scale bar,* 10 μm.

Lack of complex N-linked glycosylation impairs TRPC6 channel activity

Differences in the *N*-linked glycosylation of TRPC3 and TRPC6 have been reported to account for their different basal channel activities (83). Specifically, elimination of the second extracellular loop *N*-glycosylation site of TRPC6 converted a tightly receptor-regulated channel to a constitutively active channel. We were therefore surprised that our screen identified numerous enzymes involved in *N*-linked glycosylation as potentially contributing to the toxicity of TRPC6 GOF mutants.

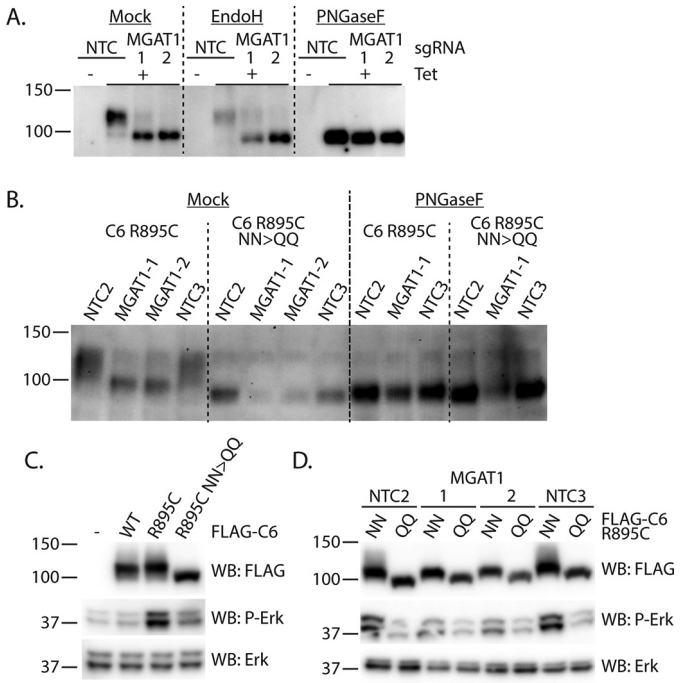

Figure 5. *N*-Linked glycosylation of TRPC6 R895C. *A,* Western blot analysis of Tet-inducible FLAG–TRPC6 R895C-expressing cells with a control CRISPR sgRNA (NTC) or with MGAT1-knockout mediated by one of two sgRNAs. Lysates were treated as indicated with EndoH (to remove immature *N*-glycans), PNGaseF (to remove all *N*-glycans), or mock-treated prior to SDS-PAGE. *B,* FLAG–TRPC6 R895C or FLAG–TRPC6 R895C carrying mutations of both *N*-glycosylation sites, N473Q and N561Q (NN → QQ), was expressed in two control (NTC) and two MGAT1 knockout cell lines. Lysates were subjected to PNGaseF treatment as indicated prior to SDS-PAGE and Western blot analysis. *C,* HEK cells transiently expressing FLAG–TRPC6 carrying the indicated mutations were lysed and subjected to Western blotting (*WB*) with the indicated antibodies. The increase in phospho-ERK levels induced by the R895C mutation was largely abrogated by the dual glycosylation site mutation. *D,* Western blot analysis of two control (NTC) and two MGAT1 knockout cell lines expressing FLAG–TRPC6 R895C with (NN) or without (QQ) *N*-glycosylation sites.

Our initial efforts to examine this discrepancy have focused on the role of MGAT1, as knockout of this enzyme had the most robust effect on rescuing cell viability (Fig. 2*C*). We confirmed by enzymatic deglycosylation that the difference in TRPC6 mobility on SDS-PAGE observed in MGAT1 knockout cells reflects the differences in *N*-glycosylation and that mature TRPC6 glycosylation normally contains hybrid or complex *N*-glycans resistant to EndoH cleavage (Fig. 5*A*). Mutation of the two previously reported (83) *N*-glycosylation sites (Asn-473 and Asn-561) to glutamine (NN → QQ) abolished the difference in gel mobility of TRPC6 expressed in control or in MGAT1-deficient cells, and it prevented further mobility shift upon PNGase treatment (Fig. 5*B*), confirming that these two asparagine residues are the only major sites of *N*-glycosylation in TRPC6. This allowed us to address whether the effects of MGAT1 knockout on TRPC6 functions are mediated directly through alterations in TRPC6 glycosylation or might reflect impaired glycosylation of other endogenous proteins.

We assayed ERK phosphorylation as a surrogate marker of mutant TRPC6 activity, as we have previously demonstrated that TRPC6 GOF mutants activate ERK in a channel-dependent manner (71). Introduction of the double glycosylation mutation into TRPC6 R895C largely abrogated the channel's ability to increase phospho-ERK levels (Fig. 5*C*). TRPC6 R895C expressed in MGAT1 knockout cells also demonstrated little ability to activate ERK (Fig. 5*D*). However, TRPC6 R895C with immature glycosylation still slightly increased phospho-ERK levels compared with TRPC6 R895C NN → QQ (Fig. 5*D*; compare *lanes 3 versus 4* and *lanes 5 versus 6*).

To more directly ascertain the role of glycosylation on TRPC6 channel function, we examined intracellular calcium influx in response to the TRPC3/6 agonist, GSK1702934A (84, 85). GSK1702934A induced an increase in Fura-2 fluorescence ratio in TRex293 cells expressing FLAG–TRPC6 R895C, but not in uninduced cells (Fig. 6, *A* and *B*). Compared with TRPC6 R895C cells with an NTC CRISPR construct, TRCP6 R895C cells with MGAT1 deletion showed a significantly diminished Fura-2 response to GSK1702934A. Whole-cell voltage– clamp experiments confirmed that TRPC6 R895C current densities in MGAT1 knockout cells were significantly lower than in control cells in response to agonist, but not at baseline (Fig. 6, *C* and *D*). Taken together, these results demonstrate that complex *N*-linked glycosylation is required for TRPC6 R895C-mediated channel activity and resultant calcium influx, ERK activation, and cytotoxicity.

Modulation of channel activity through regulation of surface expression has been reported for several TRPC channels, including TRPC6 (12, 14, 16, 86–91). To test whether glycosylation impacts surface expression of TRPC6, we compared surface biotinylation of TRPC6 R895C in control and MGAT1-deficient cells (Fig. 7*A*). As we reported previously (67), only the fully glycosylated, upper band of TRPC6 is expressed on the cell surface in control cells. However, the lower molecular weight form of TRPC6 present in MGAT1 knockout cells could be detected by surface biotinylation, with a similar ratio of surface–to–total TRPC6 R895C detected in control and MGAT1 knockout cells (Fig. 7*B*). We performed similar experiments comparing WT and the NN → QQ glycosylation-deficient TRPC6 transiently expressed in control NTC 293T cells (Fig. 7, *C* and *D*). Unlike TRPC6 with immature *N*-glycans expressed in MGAT1-knockout cells, a significantly lower ratio of TRPC6 lacking *N*-glycosylation sites was available for surface biotinylation. This was not due to the R895C mutation itself, as the NN → QQ mutation diminished surface expression of TRPC6 R895C and WT TRPC6 to similar extents (Fig. 7*C*). These results suggest that some form of *N*-linked glycosylation is required for TRPC6 surface expression, whereas MGAT1-dependent hybrid or complex *N*-glycans are required for proper TRPC6 channel activity, but not for surface expression.

TRPC6 GOF cytotoxicity in podocytes requires TRPC6 N-linked glycosylation, but not MGAT1

Podocyte injury is a central driver of FSGS pathogenesis, and podocyte-specific overexpression of TRPC6 mutants induces mild glomerular disease in mice (92). We therefore examined whether TRPC6 GOF mutations are also cytotoxic in an immortalized human podocyte cell line (93) and whether this phenotype is also dependent upon *N*-linked glycosylation. Human podocytes were transduced with lentiviral particles driving doxycycline-inducible expression of WT or R895C mutant TRPC6, with (NN) or without (QQ) *N*-linked glycosyl-

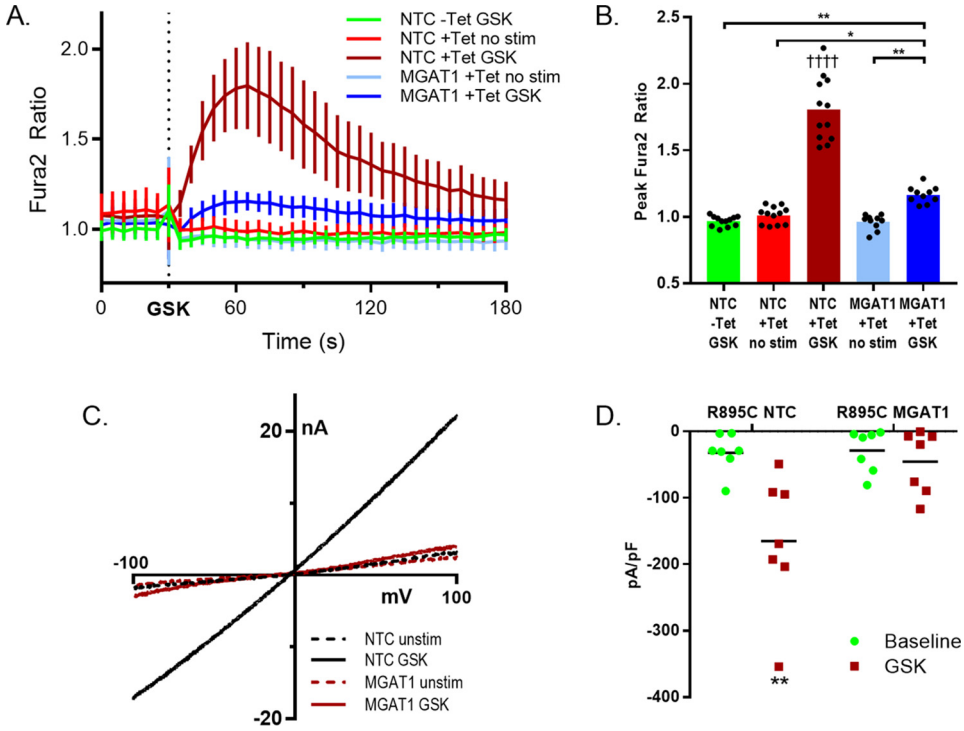

Figure 6. MGAT1 knockout diminishes TRPC6 R895C-mediated calcium influx and whole-cell current in response to GSK1702934A. *A,* time course of Fura-2 fluorescence ratio in TRex293 FLAG–TRPC6 R895C cells. Control CRISPR (NTC) or MGAT1 knockout (MGAT1) cells were treated with or without tetracycline to induce TRPC6 expression as indicated prior to Fura2 imaging. GSK1702934A (final concentration 100 μM) or DMSO vehicle control (*no stim*) was added after 30 s to activate TRPC6. Shown are means ± S.D. from $n = 10–12$ experiments performed on 3 different days. *B,* peak post-stimulation Fura2 fluorescence ratios from fluorescence traces shown in *A*; shown are the means and values from individual experiments. One-way ANOVA with Sidak's multiple comparison test; **, $p < 0.005$; *, $p < 0.05$; ††††, $p < 0.0001$ *versus* all other groups. *C, I-V* curves before (*dashed line*) and after GSK1702934A (*solid line*) stimulation of representative individual TRex293 FLAG–TRPC6 R895C cells with control CRISPR (NTC) or MGAT1 knockout (MGAT1). *D,* baseline and GSK1702934A stimulated peak current density measured at −60 mV. Shown are the means and values of each individual cell; two-way ANOVA with Sidak's multiple comparison test; **, $p < 0.005$ *versus* all other groups; all other pairwise comparisons not significant; $n = 7$ per group.

ation sites (Fig. 8*A*). Doxycycline-inducible, TRPC6 R895C-expressing podocytes were further transduced with either control (NTC) or MGAT1-targeting LentiCRISPR virus (Fig. 8*B*). TRPC6 mobility shift served to confirm the efficient loss of MGAT1 activity. Expression of TRPC6 R895C, but not of WT TRPC6 or TRPC6 R895C lacking *N*-linked glycosylation sites, significantly decreased cell viability as assessed by MTT assay (Fig. 8*C*). CRISPR-mediated knockout of MGAT1, however, failed to significantly rescue the toxicity of TRPC6 R895C expression in podocytes (Fig. 8*D*), in contrast to its effect in HEK cells (Fig. 2*C*). In sum, these results suggest that TRPC6 GOF mutants are cytotoxic in a variety of cells, including podocytes, and that this phenotype depends upon TRPC6 *N*-linked glycosylation, but that the need for MGAT1-mediated complex glycans is cell type–specific.

Discussion

Previous studies have implicated numerous signaling cascades both upstream and downstream of TRPC6 channel activity. However, the role of these pathways in the potential adverse effects of TRPC6 GOF mutations remains unclear. Based on an unbiased, genome-wide CRISPR-Cas screen, we report here that efficient TRPC6 protein expression requires the expression of several proteins, including TMEM208, and components of the EMC complex. In addition, *N*-linked glycosylation of TRPC6 was found necessary at several stages for efficient TRPC6 function. Deletion of *N*-glycosylation sites limits surface expression of TRPC6, while blocking formation of hybrid and complex *N*-glycans through loss of MGAT1 impairs TRPC6 GOF-mediated current and calcium influx without reducing TRPC6 surface expression. Interestingly, dependence on MGAT1 function, but not on *N*-glycosylation, for TRPC6 GOF cytotoxicity appears to be cell type-specific. Together, these results advance our understanding of the requirements for proper TRPC6 channel expression and function, and they establish multiple novel avenues for further investigation of TRPC6 channel regulation.

Multiple members of the EMC were identified in our screen of modulators of TRPC6 GOF toxicity, with validated hits EMC2 and EMC6 both necessary for effective TRPC6 expression. The EMC is an ER-resident multiprotein complex found in all eukaryotes (94). It functions as a transmembrane insertase required for the insertion and proper membrane topology of tail-anchored and multitransmembrane proteins (80, 95, 96), including GPCRs, transporters, and channels (81, 97, 98). Our results are in line with prior work (81) demonstrating that dPob/EMC is essential for TRP channel expression in the *Drosophila* eye.

Our data demonstrate a need for TMEM208 for the effective expression of TRPC6 and several additional polytopic transmembrane proteins. TMEM208 (hSnd2) and its yeast ortholog, Snd2, have been identified as members of an SRP-independent (SND) pathway that preferentially targets proteins with C-ter-

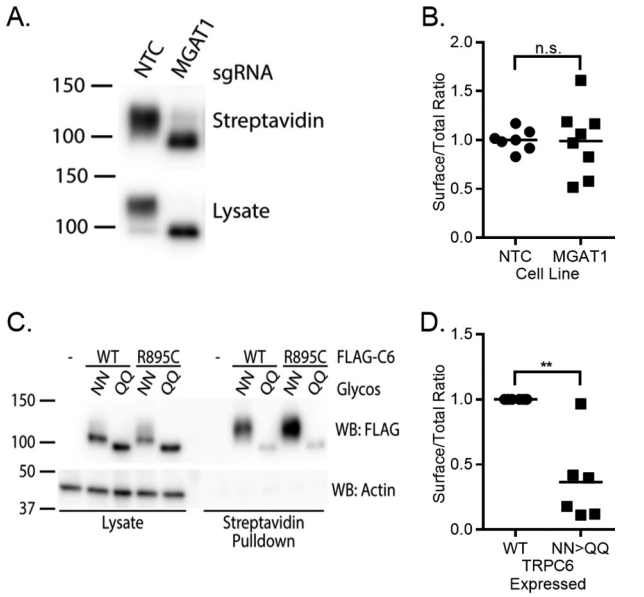

Figure 7. Surface expression of TRPC6 glycosylation mutants. *A,* control (NTC) or MGAT1 knockout (MGAT1) cells expressing Tet-inducible FLAG–TRPC6 R895C were subjected to surface biotinylation. FLAG Western blot analysis was performed on streptavidin precipitates and whole lysate. *B,* ratios of surface-accessible–to–total FLAG–TRPC6 R895C in control and MGAT1 knockout cells; $n = 7–8$; unpaired *t* test, $p = 0.943$; *n.s.*, not significant. *C,* FLAG-tagged wildtype (*WT*) or R895C mutant TRPC6 with intact (NN) or mutant (QQ) *N*-linked glycosylation sites was transiently expressed in control NTC cells. Surface-biotinylated protein was isolated by streptavidin precipitation and compared with whole lysate by Western blotting (*WB*). Actin served as a loading control and as a negative control for surface biotinylation. *D,* ratios of surface–accessible–to–total FLAG–TRPC6 WT and NN → QQ glycosylation mutant expressed in control (NTC) 293T cells; $n = 6$ per group; paired *t* test, $p = 0.0049$.

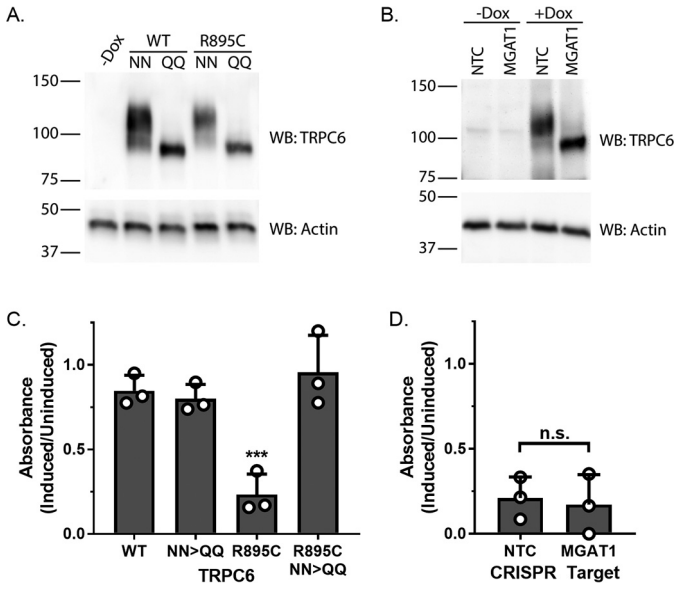

Figure 8. Role of *N*-linked glycosylation and MGAT1 function in TRPC6 R895C-mediated cytotoxicity in podocytes. *A,* Western blot (*WB*) analysis of podocytes transduced with lentivirus constructs driving doxycycline (*Dox*)-inducible expression of wildtype (WT) or R895C mutant TRPC6 with intact (NN) or mutant (QQ) *N*-linked glycosylation sites. TRPC6 expression was induced by addition of doxycycline in all samples except the *1st lane* (*−Dox*). Actin served as a loading control. *B,* doxycycline-inducible TRPC6 R895C-expressing podocytes were transduced with LentiCRISPR virus with a no target control (NTC) sgRNA or sgRNA targeting MGAT1. Lysates from cells grown in the absence or presence of doxycycline were analyzed by Western blotting for TRPC6 and actin. *C,* relative cell viability, measured as MTT assay absorbance from doxycycline-induced cells relative to uninduced cells. Podocytes expressing WT TRPC6 (WT), *N*-linked glycosylation mutant TRPC6 (NN → QQ), TRPC6 R895C mutant with intact (R895C), or mutated (R895C NN → QQ) glycosylation sites, as shown in *A*, were examined. Shown are means ± S.D. as well as individual means from each of three independent experiments; one-way ANOVA with Tukey's multiple comparisons test; ***, $p < 0.005$ *versus* all other cell lines; all other comparisons not statistically significant. *D,* relative cell viability, measured as in *C*, of control or MGAT1-knockout podocytes expressing TRPC6 R895 (as in *B*). Means ± S.D., as well as individual means from each of three independent experiments, are shown; *n.s.*, $p = 0.33$ by two-tailed, paired *t* test.

minal transmembrane domains to the ER (72, 99, 100). Mammalian homologs of the other yeast Snd components, Snd1 and Snd3, remain undefined. Previous studies have largely focused on the importance of TMEM208 for ER translocation of C-terminal single transmembrane domain proteins (99, 100). Our data suggest that TMEM208 is also required for the biosynthesis of several multipass transmembrane proteins, although delineation of the breadth of this TMEM208 requirement awaits further study. Although the loss of neither EMC2 nor EMC6 affects TMEM208 protein levels, and loss of TMEM208 does not affect EMC2 or EMC6 levels, MS data suggest a physical interaction between Snd2 and EMC1 and EMC5 (72). Thus, TMEM208 and the EMC may cooperate in the ER membrane insertion of a variety of polytopic transmembrane proteins, including TRPC6.

WDR83OS is a little studied gene that also emerged as a hit in our CRISPR screen. WDR83OS is a ubiquitously expressed, predicted transmembrane protein evolutionarily conserved in *Caenorhabditis elegans* and *Drosophila melanogaster*. It is reported to interact with the Parkinson's disease P-type ATPase ATP13A2/PARK9 (101) and with the bile acid transporter ABCB11/BSEP (102). A homozygous splice site mutation in WDR83OS has been associated with a syndrome, including hypercholanemia, intractable itching, intellectual disability, and dysmorphic features (103). Although WDR83OS knockout affects TRPC6 protein levels, and WDR83OS can interact with both TRPC6 and TMEM208, our inability to rescue TRPC6 expression by overexpressing WDR83OS in WDR83OS knockout cells prevents definitive identification of this protein as required for TRPC6 function. It will be interesting to determine whether WDR83OS knockout affects expression of other transmembrane proteins in addition to TRPC6 and to ascertain which sequences of TRPC6 are involved in binding to WDR83OS and TMEM208. In addition, the functional significance of the interaction between WDR83OS and TMEM208 will require an independent line of study.

A previous study has reported that *N*-linked glycosylation is necessary for the low basal ion channel activity of TRPC6 (83). In particular, the second extracellular loop *N*-glycosylation site (absent in the related TRPC3 channel characterized by higher basal activity) was found to mediate the tight receptor regulation of TRPC6. Deletion of this second glycosylation site, or of both glycosylation sites, did not prevent surface expression, but it enhanced basal channel activity without significantly altering peak current densities after histamine stimulation (83). We were therefore surprised to find that preventing complex *N*-glycan formation through loss of MGAT1 significantly attenuated GSK1702934A-stimulated TRPC6 R895C current and channel-dependent calcium influx, as well as GOF mutant-

induced ERK activation and cytotoxicity in HEK cells. Furthermore, mutating both *N*-glycosylation sites diminished TRPC6 surface expression and prevented TRPC6 GOF mutant-induced ERK activation, suggesting graded effects on the channel mediated by incomplete *N*-glycan maturation compared with a complete lack of glycosylation. This graded effect was most pronounced when examining the cytotoxic effect of TRPC6 R895C in podocytes. We cannot at present provide a satisfying synthesis of our results and those of Dietrich *et al.* (83). Differences in experimental design, including the use of different mechanisms to activate the channel, the presence of the R895C mutation, and different overexpression methods, are potential factors contributing to the discrepant results. It is noteworthy that in addition to MGAT1, several additional genes involved in *N*-glycan formation were identified in our initial screen, including FUT8 and SLC35C1 involved in *N*-glycan fucosylation (104), supporting the notion that *N*-glycosylation directly or indirectly modulates TRPC6 activity.

We utilized the cytotoxic phenotype of overexpressed gain–of–function TRPC6 mutants to perform our screen agnostic as to the mechanism. We speculate that the cytotoxicity is due to calcium overload, as we have previously noted increased intracellular calcium levels in our Tet-inducible HEK cells (67, 71), and calcium overload is known to activate multiple forms of cell death, including apoptosis and necrosis (105). The presence of FADD and TNFRSF10B in our initial list of screen hits suggests death receptor-mediated apoptotic signaling (106) may be involved. These hypotheses are being tested by ongoing experiments. Ultimately, the question of whether TRPC6 GOF-mediated cytotoxicity is involved in the development of FSGS will require testing in a robust model of the disease, one currently unavailable.

In summary, exploiting the cytotoxic effects of overexpressed TRPC6 GOF mutants, we have identified several biological processes necessary for TRPC6 expression and function. In addition to an expected role for EMC in TRPC6 expression, we have identified TMEM208 as a necessary factor for the expression of several polytopic transmembrane proteins, including TRPC6, thus expanding the role of the human homolog of SND2. Our results further suggest that *N*-glycosylation plays a critical role in TRPC6 function, affecting both surface expression and ion channel function. These findings imply a more complex role for glycosylation in the function and regulation of TRPC6 than previously envisioned. In addition, it is tempting to speculate that tissue- or cell type–specific glycosylation may influence channel activity, possibly contributing to the renal-limited phenotype of human TRPC6 mutations. A more detailed examination of these hypotheses will be the focus of future studies.

Experimental procedures

Reagents and plasmids

TRex293 (Invitrogen) stable cell lines expressing FLAG-tagged TRPC6 WT, R895C, and E897K mutant channels were previously described (67), as were N-terminal FLAG- and HA-tagged TRPC6 expression constructs (71). Conditionally immortalized human podocytes were maintained as described previously (93). LentiCRISPR v2 (107), lentiCas9-Blast (74), pCW57-MCS1-P2A-MCS2(Blast) (108), psPAX2, and pCMV-VSV-G (109) plasmids were from Addgene (plasmids 52961, 52962, 80921, 12260, and 8454, respectively). Human TMEM208 and WDR83OS expression constructs in pLX304 (110) were from the Harvard Medical School PlasmID Repository (clones HsCD00420103 and HsCD00421132, respectively). Expression constructs for WDR83OS and TMEM208 tagged with C-terminal V5, HA, or FLAG were created by G-block cloning into pcDNA3.1 Myc/His A (Invitrogen). The cDNA was made Cas9-resistant by mutating the PAM site for each CRISPR guide while maintaining the protein-coding sequence. The human TRPC6 ORF with various GOF and glycosylation mutations was subcloned into pCW57 digested with NheI and BamHI using HiFi DNA assembly. Restriction enzymes, Hi-Fi master mix, stable-competent *Escherichia coli*, PNGaseF, and EndoH were from New England Biolabs. Antibodies were from the following sources: Cell Signaling Technology (rabbit phospho-ERK1/2, catalog no. 4370; rabbit ERK1/2, catalog no. 4695; rabbit and mouse anti-HA antibodies, catalog nos. 3724 and 2367; horseradish peroxidase–conjugated anti-rabbit and anti-mouse IgG secondary antibodies, catalog nos. 7074 and 7076); Proteintech (rabbit anti-TMEM208 antibody, 23882-1-AP); Sigma (unconjugated (F3165) and agarose-coupled (A2220) FLAG M2, HA mouse monoclonal conjugated to agarose (A2095)); and Thermo Fisher Scientific (V5 tag mAb E10/V4RR; WDR83OS polyclonal antibody PA5-66788). Fluorescence-conjugated secondary antibodies and phalloidin were from Jackson ImmunoResearch and Invitrogen, respectively. Oligonucleotides and G-blocks were from IDT. Tissue culture media were from Mediatech; tetracycline-free fetal bovine serum was from Atlanta Biologicals. GSK1702934A was from Focus Biomolecules. X-tremeGENE 9 transfection reagent was from Sigma.

Lentiviral transduction

HEK293T cells (ATCC CRL-3216) were transiently transfected using X-tremeGENE 9 with psPAX2, pCMV-VSV-G, and either LentiCRISPR v2 or pCW57 constructs in a 2:1:3 weight/weight ratio. After 6 h, fresh media were applied. Conditioned media containing viral particles were collected and cleared by centrifugation every 24 h for 2 days. Human podocytes were transduced by incubating with virally conditioned media and hexadimethrine bromide (8 μg/ml) overnight, followed by selection with either 30 μg/ml blasticidin or 1 μg/ml puromycin.

Cell proliferation and cytotoxicity studies

Freshly trypsinized cells were counted and plated as indicated. Cells were cultured in complete media in the absence or presence of 50 ng/ml tetracycline or 1 μg/ml doxycycline to induce TRPC6 expression. For assessment of cell viability by MTT, cells were plated at 5×10^3 cells per well in a 96-well plate and grown with or without tetracycline, or doxycycline, in complete media for 96 h. Media were replaced with dye-free complete media containing MTT (0.5 mg/ml), and cells were incubated at 37 °C for 3 h. After removal of media, MTT crystals were solubilized in 0.1 N HCl in isopropyl alcohol, and absor-

bance was measured at 570 nm with background at 660 nm (SpectraMax5, Molecular Devices). For cytotoxicity and viability measurements using the MultiTox-Fluor Multiplex Cytotoxicity assay (Promega), 10^5 cells were plated per well of a 96-well plate and grown with or without tetracycline in complete media for 24 h. Toxicity was then assayed per the manufacturer's protocol.

Genome-wide CRISPR screen

Lentivirus containing the Brunello human CRISPR knockout pooled plasmid library (74) in the lentiGuide-Puro backbone was obtained from Addgene (catalog no. 73178-LV). The positive selection screen and amplification of integrated sgRNA sequences were performed as outlined in Ref. 74, with minor adjustments. Briefly, stable Tet-inducible TRPC6 E897K-expressing TRex 293 cells (67) were first transduced with lenti-Cas9-Blast. Approximately 9×10^7 cells were then infected with the Brunello CRISPR knockout library at a multiplicity of infection of 0.35, followed by selection with puromycin (1 μg/ml). This provided an estimated representation of 400 cells per sgRNA. After 7 days of puromycin selection cells were trypsinized, and ~25% of the cell population (8.5×10^7 cells) was harvested for Next Generation Illumina sequencing. The remainder (2.6×10^8 cells) was treated with tetracycline (50 ng/ml) to induce TRPC6 E897K expression, resulting in a cytotoxic phenotype. After 2 weeks culture in the presence of TRPC6 E897K induction, surviving cells were harvested, and genomic DNA was isolated. Guide RNA amplification and preparation for sequencing were performed using established protocols (74). Next Generation Sequencing was performed on an Illumina MiSeq machine. Read mapping and sgRNA enrichment was performed using the online CRISPR AnalyzeR (http://crispr-analyzer.dkfz.de/).[3]

Validation of CRISPR screen hits

CRISPR knockout cells were made for each of the target genes chosen for further study. TRex293 cells expressing the Tet-inducible mutant TRPC6 R895C were transfected with the LentiCRISPR v2 plasmid containing one of two distinct sgRNAs for the target gene, followed by selection with puromycin (2 μg/ml). To confirm rescue of the TRPC6 R895C-induced cytotoxic phenotype, the CRISPR KO TRPC6 R895C cells were treated with tetracycline to induce TRPC6 R895C expression for 90 h. Cell viability was quantified by MTT assay. FLAG–TRPC6 expression was evaluated by Western blotting.

Calcium fluorescence ratio measurement

TRPC6 channel activity was assessed by Fura-2 fluorescence ratio measurement of intracellular calcium ion (Fura-2 QBT kit, Molecular Devices, catalog no. R8197) in a 96-well format on a FlexStation 3 microplate reader with automated pipetting at the Harvard ICCB-Longwood screening facility. Cells were incubated with the Fura-2 dye for 1 h at 37 °C and then excited every 5 s at wavelengths of 340 and 380 nm, with Fura-2 fluorescence emission read at 510 nm. Agonist or vehicle carrier was added after 30 s. Digitonin was added at the end of every experiment as a positive control for dye loading.

Electrophysiology

FLAG–TRPC6 R895C– expressing TRex293 stable cell lines transfected with control or MGAT1-targeting LentiCRISPR were grown on coverslips and mounted on an inverted microscope in a 200-μl open chamber (WPI, Sarasota, FL). Patch pipettes of resistance 1.5–3 megohms were filled with a solution consisting of (in mM): 140 Cs methanesulfonate, 10 EGTA, 10 HEPES, 2.27 $MgCl_2$, 1.91 $CaCl_2$, and 1 NaATP, pH 7.2, with CsOH. The bath solution contained (in mM): 145 NaCl, 5 KCl, 1 $MgCl_2$, 2 $CaCl_2$, 10 HEPES, and 10 glucose, pH 7.4, with NaOH. Whole-cell patch currents were recorded (Axopatch 200, Molecular Devices, Sunnyvale, CA) and digitized with a 1550B AD/DA board (Molecular Devices). To determine current–voltage relationships (*I-V* curves) in Clampex (pClamp11, Molecular Devices), a 500-ms ramp protocol from +100 to −100 mV was repeated every 10 s for the duration of the experiment (111). The bath reference electrode was a silver chloride wire with a 3 M KCl agar bridge. Data were filtered at 500 Hz, digitized at 10 kHz by Clampex, and analyzed offline by Clampfit subroutine (pClamp11). Holding potentials in whole-cell patch experiments were expressed as V_m, the pipette potential. The ramp current measured at −60 mV was chosen to report whole-cell conductance.

Immunoprecipitation and Western blotting

Experiments were performed essentially as described previously (71). After removing media and rinsing cells in cold PBS, cells were lysed in TBS (50 mM Tris-HCl, pH 7.4, 150 mM NaCl) containing 1% (v/v) Nonidet P-40, EDTA-free Complete protease inhibitor, and PhosStop (Roche Applied Science). Lysates were cleared by centrifugation at 17,000 × *g* for 15 min at 4 °C. An aliquot was mixed with 4× SDS-sample loading buffer with β-mercaptoethanol, incubated at 95 °C for 5 min, and used to assay protein expression by Western blotting.

For immunoprecipitation, cleared lysates were incubated with 20 μl of FLAG M2 or anti-HA-agarose slurry and incubated with constant agitation at 4 °C for 2–3 h. Immunoprecipitated complexes were washed three times with lysis buffer and eluted by boiling in SDS sample loading buffer.

Mini-PROTEAN TGX and Tris-Tricine gels (Bio-Rad) were utilized for SDS-PAGE, followed by transfer onto polyvinylidene difluoride membrane for immunoblotting as described previously (71).

Surface biotinylation assay

Cells were washed with HBSS and incubated with 1 mg/ml sulfo-NHS-SS-biotin (Thermo Fisher Scientific catalog no. 21331) at 4 °C for 1 h. The reaction was quenched with 5 mM Tris in HBSS, and cells were lysed in TBS 1% Nonidet P-40. Lysate was incubated with streptavidin-agarose beads at 4 °C for 2 h. Beads were washed, and biotinylated protein was eluted in sample loading buffer for Western blotting.

TRPC6 glycosylation mutants

The two known TRPC6 *N*-glycosylation sites (Asn-473 and Asn-561) were mutated to glutamine residues in the FLAG–

[3] Please note that the JBC is not responsible for the long-term archiving and maintenance of this site or any other third party hosted site.

hTRPC6 expression constructs using the QuikChange II XL site-directed mutagenesis kit (Agilent Technologies catalog no. 200521). Successful mutation was confirmed by Sanger sequencing. FLAG–TRPC6 WT or NN → QQ mutant was transfected into CRISPR NTC cells or into CRISPR MGAT1 knockout 293T cells. Differences in TRPC6 glycosylation were visualized by mobility shift on SDS-PAGE. Western blotting was also used to identify alterations in p-ERK levels.

Immunocytochemistry

HeLa cells were transfected with expression plasmids encoding FLAG–TRPC6 and V5-WDR83OS or FLAG–WDR83OS and V5-TMEM208. After 24 h, cells were fixed in 4% paraformaldehyde and 4% sucrose in PBS and permeabilized at room temperature with 0.3% Triton X-100 in PBS. Cells were blocked with PBS containing 2% fetal bovine serum, 2% BSA, 0.2% fish gelatin for 1 h, followed by a 2-h incubation with primary antibody directed against FLAG and V5. After rinsing, cells were incubated with secondary antibody for 1 h before mounting. Confocal images were obtained on a Zeiss LSM510 upright confocal system at the Beth Israel Deaconess Confocal Imaging Core.

Author contributions—B. E. T., D. H. V., B. R. S., and J. S. S. investigation; B. E. T. and D. H. V. methodology; B. E. T., D. H. V., and J. S. S. writing-original draft; S. L. A. resources; S. L. A. and J. S. S. supervision; S. L. A. and J. S. S. writing-review and editing; J. S. S. conceptualization; J. S. S. funding acquisition.

Acknowledgments—We thank the Beth Israel Deaconess Medical Center Molecular Medicine, Confocal Imaging, and Flow Cytometry Cores, and the Harvard ICCB-Longwood Screening Core, for technical assistance and expertise. We are indebted to the multiple researchers who made their plasmids available. We are grateful to Martin Pollak and members of his laboratory for thoughtful discussions and suggestions.

References

1. Ramsey, I. S., Delling, M., and Clapham, D. E. (2006) An introduction to TRP channels. *Annu. Rev. Physiol.* **68,** 619–647 CrossRef Medline
2. Nilius, B., and Voets, T. (2005) TRP channels: a TR(I)P through a world of multifunctional cation channels. *Pflugers Arch.* **451,** 1–10 CrossRef Medline
3. Hofmann, T., Obukhov, A. G., Schaefer, M., Harteneck, C., Gudermann, T., and Schultz, G. (1999) Direct activation of human TRPC6 and TRPC3 channels by diacylglycerol. *Nature* **397,** 259–263 CrossRef Medline
4. Goel, M., Sinkins, W. G., and Schilling, W. P. (2002) Selective association of TRPC channel subunits in rat brain synaptosomes. *J. Biol. Chem.* **277,** 48303–48310 CrossRef Medline
5. Hofmann, T., Schaefer, M., Schultz, G., and Gudermann, T. (2002) Subunit composition of mammalian transient receptor potential channels in living cells. *Proc. Natl. Acad. Sci. U.S.A.* **99,** 7461–7466 CrossRef Medline
6. Schilling, W. P., and Goel, M. (2004) Mammalian TRPC channel subunit assembly. *Novartis Found. Symp.* **258,** 18–30 Medline
7. Bouron, A., Chauvet, S., Dryer, S., and Rosado, J. A. (2016) Second messenger-operated calcium entry through TRPC6. *Adv. Exp. Med. Biol.* **898,** 201–249 CrossRef Medline
8. Basora, N., Boulay, G., Bilodeau, L., Rousseau, E., and Payet, M. D. (2003) 20-Hydroxyeicosatetraenoic acid (20-HETE) activates mouse TRPC6 channels expressed in HEK293 cells. *J. Biol. Chem.* **278,** 31709–31716 CrossRef Medline
9. Inoue, R., Jensen, L. J., Jian, Z., Shi, J., Hai, L., Lurie, A. I., Henriksen, F. H., Salomonsson, M., Morita, H., Kawarabayashi, Y., Mori, M., Mori, Y., and Ito, Y. (2009) Synergistic activation of vascular TRPC6 channel by receptor and mechanical stimulation via phospholipase C/diacylglycerol and phospholipase A2/ω-hydroxylase/20-HETE pathways. *Circ. Res.* **104,** 1399–1409 CrossRef Medline
10. Roshanravan, H., Kim, E. Y., and Dryer, S. E. (2016) 20-Hydroxyeicosatetraenoic acid (20-HETE) modulates canonical transient receptor potential-6 (TRPC6) channels in podocytes. *Front. Physiol.* **7,** 351 CrossRef Medline
11. Boulay, G., Zhu, X., Peyton, M., Jiang, M., Hurst, R., Stefani, E., and Birnbaumer, L. (1997) Cloning and expression of a novel mammalian homolog of *Drosophila* transient receptor potential (Trp) involved in calcium entry secondary to activation of receptors coupled by the G_q class of G protein. *J. Biol. Chem.* **272,** 29672–29680 CrossRef Medline
12. Cayouette, S., Lussier, M. P., Mathieu, E. L., Bousquet, S. M., and Boulay, G. (2004) Exocytotic insertion of TRPC6 channel into the plasma membrane upon G_q protein-coupled receptor activation. *J. Biol. Chem.* **279,** 7241–7246 CrossRef Medline
13. Hisatsune, C., Kuroda, Y., Nakamura, K., Inoue, T., Nakamura, T., Michikawa, T., Mizutani, A., and Mikoshiba, K. (2004) Regulation of TRPC6 channel activity by tyrosine phosphorylation. *J. Biol. Chem.* **279,** 18887–18894 CrossRef Medline
14. Kim, E. Y., Anderson, M., and Dryer, S. E. (2012) Insulin increases surface expression of TRPC6 channels in podocytes: role of NADPH oxidases and reactive oxygen species. *Am. J. Physiol. Renal Physiol.* **302,** F298–F307 CrossRef Medline
15. Kanda, S., Harita, Y., Shibagaki, Y., Sekine, T., Igarashi, T., Inoue, T., and Hattori, S. (2011) Tyrosine phosphorylation-dependent activation of TRPC6 regulated by PLC-γ1 and nephrin: effect of mutations associated with focal segmental glomerulosclerosis. *Mol. Biol. Cell* **22,** 1824–1835 CrossRef Medline
16. Graham, S., Ding, M., Ding, Y., Sours-Brothers, S., Luchowski, R., Gryczynski, Z., Yorio, T., Ma, H., and Ma, R. (2010) Canonical transient receptor potential 6 (TRPC6), a redox-regulated cation channel. *J. Biol. Chem.* **285,** 23466–23476 CrossRef Medline
17. Ding, Y., Winters, A., Ding, M., Graham, S., Akopova, I., Muallem, S., Wang, Y., Hong, J. H., Gryczynski, Z., Yang, S. H., Birnbaumer, L., and Ma, R. (2011) Reactive oxygen species-mediated TRPC6 protein activation in vascular myocytes, a mechanism for vasoconstrictor-regulated vascular tone. *J. Biol. Chem.* **286,** 31799–31809 CrossRef Medline
18. Liu, B. C., Song, X., Lu, X. Y., Li, D. T., Eaton, D. C., Shen, B. Z., Li, X. Q., and Ma, H. P. (2013) High glucose induces podocyte apoptosis by stimulating TRPC6 via elevation of reactive oxygen species. *Biochim. Biophys. Acta* **1833,** 1434–1442 CrossRef Medline
19. Kim, E. Y., Anderson, M., and Dryer, S. E. (2012) Sustained activation of *N*-methyl-D-aspartate receptors in podoctyes leads to oxidative stress, mobilization of transient receptor potential canonical 6 channels, nuclear factor of activated T cells activation, and apoptotic cell death. *Mol. Pharmacol.* **82,** 728–737 CrossRef Medline
20. Spassova, M. A., Hewavitharana, T., Xu, W., Soboloff, J., and Gill, D. L. (2006) A common mechanism underlies stretch activation and receptor activation of TRPC6 channels. *Proc. Natl. Acad. Sci. U.S.A.* **103,** 16586–16591 CrossRef Medline
21. Mederos y Schnitzler, M., Storch, U., Meibers, S., Nurwakagari, P., Breit, A., Essin, K., Gollasch, M., and Gudermann, T. (2008) G_q-coupled receptors as mechanosensors mediating myogenic vasoconstriction. *EMBO J.* **27,** 3092–3103 CrossRef Medline
22. Gottlieb, P., Folgering, J., Maroto, R., Raso, A., Wood, T. G., Kurosky, A., Bowman, C., Bichet, D., Patel, A., Sachs, F., Martinac, B., Hamill, O. P., and Honoré, E. (2008) Revisiting TRPC1 and TRPC6 mechanosensitivity. *Pflugers Arch.* **455,** 1097–1103 CrossRef Medline
23. Nikolova-Krstevski, V., Wagner, S., Yu, Z. Y., Cox, C. D., Cvetkovska, J., Hill, A. P., Huttner, I. G., Benson, V., Werdich, A. A., MacRae, C., Feneley, M. P., Friedrich, O., Martinac, B., and Fatkin, D. (2017) Endocardial TRPC-6 channels act as atrial mechanosensors and load-dependent modulators of endocardial/myocardial cross-talk. *JACC Basic Transl. Sci.* **2,** 575–590 CrossRef Medline
24. Gonzales, A. L., Yang, Y., Sullivan, M. N., Sanders, L., Dabertrand, F., Hill-Eubanks, D. C., Nelson, M. T., and Earley, S. (2014) A PLCγ1-de-

pendent, force-sensitive signaling network in the myogenic constriction of cerebral arteries. *Sci. Signal.* **7,** ra49 CrossRef Medline
25. Alessandri-Haber, N., Dina, O. A., Chen, X., and Levine, J. D. (2009) TRPC1 and TRPC6 channels cooperate with TRPV4 to mediate mechanical hyperalgesia and nociceptor sensitization. *J. Neurosci.* **29,** 6217–6228 CrossRef Medline
26. Welsh, D. G., Morielli, A. D., Nelson, M. T., and Brayden, J. E. (2002) Transient receptor potential channels regulate myogenic tone of resistance arteries. *Circ. Res.* **90,** 248–250 CrossRef Medline
27. Quick, K., Zhao, J., Eijkelkamp, N., Linley, J. E., Rugiero, F., Cox, J. J., Raouf, R., Gringhuis, M., Sexton, J. E., Abramowitz, J., Taylor, R., Forge, A., Ashmore, J., Kirkwood, N., Kros, C. J., *et al.* (2012) TRPC3 and TRPC6 are essential for normal mechanotransduction in subsets of sensory neurons and cochlear hair cells. *Open Biol.* **2,** 120068 CrossRef Medline
28. Dyachenko, V., Husse, B., Rueckschloss, U., and Isenberg, G. (2009) Mechanical deformation of ventricular myocytes modulates both TRPC6 and Kir2.3 channels. *Cell Calcium* **45,** 38–54 CrossRef Medline
29. Anderson, M., Kim, E. Y., Hagmann, H., Benzing, T., and Dryer, S. E. (2013) Opposing effects of podocin on the gating of podocyte TRPC6 channels evoked by membrane stretch or diacylglycerol. *Am. J. Physiol. Cell Physiol.* **305,** C276–C289 CrossRef Medline
30. Gudermann, T., Mederos y Schnitzler, M., and Dietrich, A. (2004) Receptor-operated cation entry–more than esoteric terminology? *Sci. STKE* 2004, pe35 CrossRef Medline
31. Estacion, M., Sinkins, W. G., Jones, S. W., Applegate, M. A., and Schilling, W. P. (2006) Human TRPC6 expressed in HEK 293 cells forms non-selective cation channels with limited Ca^{2+} permeability. *J. Physiol.* **572,** 359–377 CrossRef Medline
32. Soboloff, J., Spassova, M., Xu, W., He, L. P., Cuesta, N., and Gill, D. L. (2005) Role of endogenous TRPC6 channels in Ca^{2+} signal generation in A7r5 smooth muscle cells. *J. Biol. Chem.* **280,** 39786–39794 CrossRef Medline
33. Lemos, V. S., Poburko, D., Liao, C. H., Cole, W. C., and van Breemen, C. (2007) Na^+ entry via TRPC6 causes Ca^{2+} entry via NCX reversal in ATP stimulated smooth muscle cells. *Biochem. Biophys. Res. Commun.* **352,** 130–134 CrossRef Medline
34. Dietrich, A., and Gudermann, T. (2014) TRPC6: physiological function and pathophysiological relevance. *Handb. Exp. Pharmacol.* **222,** 157–188 CrossRef Medline
35. Kuwahara, K., Wang, Y., McAnally, J., Richardson, J. A., Bassel-Duby, R., Hill, J. A., and Olson, E. N. (2006) TRPC6 fulfills a calcineurin signaling circuit during pathologic cardiac remodeling. *J. Clin. Invest.* **116,** 3114–3126 CrossRef Medline
36. Onohara, N., Nishida, M., Inoue, R., Kobayashi, H., Sumimoto, H., Sato, Y., Mori, Y., Nagao, T., and Kurose, H. (2006) TRPC3 and TRPC6 are essential for angiotensin II-induced cardiac hypertrophy. *EMBO J.* **25,** 5305–5316 CrossRef Medline
37. Wu, X., Eder, P., Chang, B., and Molkentin, J. D. (2010) TRPC channels are necessary mediators of pathologic cardiac hypertrophy. *Proc. Natl. Acad. Sci. U.S.A.* **107,** 7000–7005 CrossRef Medline
38. Yao, H., Peng, F., Fan, Y., Zhu, X., Hu, G., and Buch, S. J. (2009) TRPC channel-mediated neuroprotection by PDGF involves Pyk2/ERK/CREB pathway. *Cell Death Differ.* **16,** 1681–1693 CrossRef Medline
39. Tai, Y., Feng, S., Ge, R., Du, W., Zhang, X., He, Z., and Wang, Y. (2008) TRPC6 channels promote dendritic growth via the CaMKIV-CREB pathway. *J. Cell Sci.* **121,** 2301–2307 CrossRef Medline
40. Zhou, J., Du, W., Zhou, K., Tai, Y., Yao, H., Jia, Y., Ding, Y., and Wang, Y. (2008) Critical role of TRPC6 channels in the formation of excitatory synapses. *Nat. Neurosci.* **11,** 741–743 CrossRef Medline
41. Tian, D., Jacobo, S. M., Billing, D., Rozkalne, A., Gage, S. D., Anagnostou, T., Pavenstädt, H., Pavenstaedt, H., Hsu, H. H., Schlondorff, J., Ramos, A., and Greka, A. (2010) Antagonistic regulation of actin dynamics and cell motility by TRPC5 and TRPC6 channels. *Sci. Signal.* **3,** ra77 CrossRef Medline
42. Singh, I., Knezevic, N., Ahmmed, G. U., Kini, V., Malik, A. B., and Mehta, D. (2007) $G\alpha_q$-TRPC6-mediated Ca^{2+} entry induces RhoA activation and resultant endothelial cell shape change in response to thrombin. *J. Biol. Chem.* **282,** 7833–7843 CrossRef Medline
43. Jiang, L., Ding, J., Tsai, H., Li, L., Feng, Q., Miao, J., and Fan, Q. (2011) Over-expressing transient receptor potential cation channel 6 in podocytes induces cytoskeleton rearrangement through increases of intracellular Ca^{2+} and RhoA activation. *Exp. Biol. Med.* **236,** 184–193 CrossRef Medline
44. Verheijden, K. A. T., Sonneveld, R., Bakker-van Bebber, M., Wetzels, J. F. M., van der Vlag, J., and Nijenhuis, T. (2018) The calcium-dependent protease calpain-1 links TRPC6 activity to podocyte injury. *J. Am. Soc. Nephrol.* **29,** 2099–2109 CrossRef Medline
45. Riccio, A., Medhurst, A. D., Mattei, C., Kelsell, R. E., Calver, A. R., Randall, A. D., Benham, C. D., and Pangalos, M. N. (2002) mRNA distribution analysis of human TRPC family in CNS and peripheral tissues. *Brain Res. Mol. Brain Res.* **109,** 95–104 CrossRef Medline
46. Beech, D. J., Muraki, K., and Flemming, R. (2004) Non-selective cationic channels of smooth muscle and the mammalian homologues of *Drosophila* TRP. *J. Physiol.* **559,** 685–706 CrossRef Medline
47. Davis, J., Burr, A. R., Davis, G. F., Birnbaumer, L., and Molkentin, J. D. (2012) A TRPC6-dependent pathway for myofibroblast transdifferentiation and wound healing *in vivo*. *Dev. Cell* **23,** 705–715 CrossRef Medline
48. Hofmann, K., Fiedler, S., Vierkotten, S., Weber, J., Klee, S., Jia, J., Zwickenpflug, W., Flockerzi, V., Storch, U., Yildirim, A. Ö., Gudermann, T., Königshoff, M., and Dietrich, A. (2017) Classical transient receptor potential 6 (TRPC6) channels support myofibroblast differentiation and development of experimental pulmonary fibrosis. *Biochim Biophys. Acta Mol. Basis Dis.* **1863,** 560–568 CrossRef Medline
49. Wu, Y. L., Xie, J., An, S. W., Oliver, N., Barrezueta, N. X., Lin, M. H., Birnbaumer, L., and Huang, C. L. (2017) Inhibition of TRPC6 channels ameliorates renal fibrosis and contributes to renal protection by soluble klotho. *Kidney Int.* **91,** 830–841 CrossRef Medline
50. Inoue, R., Kurahara, L. H., and Hiraishi, K. (2018) TRP channels in cardiac and intestinal fibrosis. *Semin. Cell Dev. Biol. 2018,* S1084-9521(18)30045-4 CrossRef Medline
51. Weissmann, N., Sydykov, A., Kalwa, H., Storch, U., Fuchs, B., Mederos y Schnitzler, M., Brandes, R. P., Grimminger, F., Meissner, M., Freichel, M., Offermanns, S., Veit, F., Pak, O., Krause, K. H., Schermuly, R. T., *et al.* (2012) Activation of TRPC6 channels is essential for lung ischaemia-reperfusion induced oedema in mice. *Nat. Commun.* **3,** 649 CrossRef Medline
52. Ilatovskaya, D. V., Blass, G., Palygin, O., Levchenko, V., Pavlov, T. S., Grzybowski, M. N., Winsor, K., Shuyskiy, L. S., Geurts, A. M., Cowley, A. W., Jr., Birnbaumer, L., and Staruschenko, A. (2018) A NOX4/TRPC6 pathway in podocyte calcium regulation and renal damage in diabetic kidney disease. *J. Am. Soc. Nephrol.* **29,** 1917–1927 CrossRef Medline
53. Spires, D., Ilatovskaya, D. V., Levchenko, V., North, P. E., Geurts, A. M., Palygin, O., and Staruschenko, A. (2018) Protective role of Trpc6 knockout in the progression of diabetic kidney disease. *Am. J. Physiol. Renal Physiol.* **315,** F1091–F1097 CrossRef Medline
54. Wang, L., Chang, J. H., Buckley, A. F., and Spurney, R. F. (2019) Knockout of TRPC6 promotes insulin resistance and exacerbates glomerular injury in Akita mice. *Kidney Int.* **95,** 321–332 CrossRef Medline
55. Kim, E. Y., Shotorbani, P. Y., and Dryer, S. E. (2019) TRPC6 inactivation does not affect loss of renal function in nephrotoxic serum glomerulonephritis in rats, but reduces severity of glomerular lesions. *Biochem. Biophys. Rep.* **17,** 139–150 CrossRef Medline
56. Kistler, A. D., Singh, G., Altintas, M. M., Yu, H., Fernandez, I. C., Gu, C., Wilson, C., Srivastava, S. K., Dietrich, A., Walz, K., Kerjaschki, D., Ruiz, P., Dryer, S., Sever, S., Dinda, A. K., *et al.* (2013) Transient receptor potential channel 6 (TRPC6) protects podocytes during complement-mediated glomerular disease. *J. Biol. Chem.* **288,** 36598–36609 CrossRef Medline
57. Du, W., Huang, J., Yao, H., Zhou, K., Duan, B., and Wang, Y. (2010) Inhibition of TRPC6 degradation suppresses ischemic brain damage in rats. *J. Clin. Invest.* **120,** 3480–3492 CrossRef Medline
58. Jia, Y., Zhou, J., Tai, Y., and Wang, Y. (2007) TRPC channels promote cerebellar granule neuron survival. *Nat. Neurosci.* **10,** 559–567 CrossRef Medline
59. Weber, E. W., Han, F., Tauseef, M., Birnbaumer, L., Mehta, D., and Muller, W. A. (2015) TRPC6 is the endothelial calcium channel that

regulates leukocyte transendothelial migration during the inflammatory response. *J. Exp. Med.* **212,** 1883–1899 CrossRef Medline
60. Damann, N., Owsianik, G., Li, S., Poll, C., and Nilius, B. (2009) The calcium-conducting ion channel transient receptor potential canonical 6 is involved in macrophage inflammatory protein-2-induced migration of mouse neutrophils. *Acta. Physiol.* **195,** 3–11 CrossRef Medline
61. Winn, M. P., Conlon, P. J., Lynn, K. L., Farrington, M. K., Creazzo, T., Hawkins, A. F., Daskalakis, N., Kwan, S. Y., Ebersviller, S., Burchette, J. L., Pericak-Vance, M. A., Howell, D. N., Vance, J. M., and Rosenberg, P. B. (2005) A mutation in the TRPC6 cation channel causes familial focal segmental glomerulosclerosis. *Science* **308,** 1801–1804 CrossRef Medline
62. Reiser, J., Polu, K. R., Möller, C. C., Kenlan, P., Altintas, M. M., Wei, C., Faul, C., Herbert, S., Villegas, I., Avila-Casado, C., McGee, M., Sugimoto, H., Brown, D., Kalluri, R., Mundel, P., Smith, P. L., *et al.* (2005) TRPC6 is a glomerular slit diaphragm-associated channel required for normal renal function. *Nat. Genet.* **37,** 739–744 CrossRef Medline
63. Heeringa, S. F., Möller, C. C., Du, J., Yue, L., Hinkes, B., Chernin, G., Vlangos, C. N., Hoyer, P. F., Reiser, J., and Hildebrandt, F. (2009) A novel TRPC6 mutation that causes childhood FSGS. *PLoS One* **4,** e7771 CrossRef Medline
64. Riehle, M., Büscher, A. K., Gohlke, B. O., Kassmann, M., Kolatsi-Joannou, M., Bräsen, J. H., Nagel, M., Becker, J. U., Winyard, P., Hoyer, P. F., Preissner, R., Krautwurst, D., Gollasch, M., Weber, S., and Harteneck, C. (2016) TRPC6 G757D loss–of–function mutation associates with FSGS. *J. Am. Soc. Nephrol.* **27,** 2771–2783 CrossRef Medline
65. Gigante, M., Caridi, G., Montemurno, E., Soccio, M., d'Apolito, M., Cerullo, G., Aucella, F., Schirinzi, A., Emma, F., Massella, L., Messina, G., De Palo, T., Ranieri, E., Ghiggeri, G. M., and Gesualdo, L. (2011) TRPC6 mutations in children with steroid-resistant nephrotic syndrome and atypical phenotype. *Clin. J. Am. Soc. Nephrol.* **6,** 1626–1634 CrossRef Medline
66. Wilson, C., and Dryer, S. E. (2014) A mutation in TRPC6 channels abolishes their activation by hypoosmotic stretch but does not affect activation by diacylglycerol or G protein signaling cascades. *Am. J. Physiol. Renal Physiol.* **306,** F1018–F1025 CrossRef Medline
67. Schlöndorff, J., Del Camino, D., Carrasquillo, R., Lacey, V., and Pollak, M. R. (2009) TRPC6 mutations associated with focal segmental glomerulosclerosis cause constitutive activation of NFAT-dependent transcription. *Am. J. Physiol. Cell Physiol.* **296,** C558–C569 CrossRef Medline
68. Hofstra, J. M., Lainez, S., van Kuijk, W. H., Schoots, J., Baltissen, M. P., Hoefsloot, L. H., Knoers, N. V., Berden, J. H., Bindels, R. J., van der Vlag, J., Hoenderop, J. G., Wetzels, J. F., and Nijenhuis, T. (2013) New TRPC6 gain–of–function mutation in a non-consanguineous Dutch family with late-onset focal segmental glomerulosclerosis. *Nephrol. Dial. Transpl.* **28,** 1830–1838 CrossRef
69. Azumaya, C. M., Sierra-Valdez, F., Cordero-Morales, J. F., and Nakagawa, T. (2018) Cryo-EM structure of the cytoplasmic domain of murine transient receptor potential cation channel subfamily C member 6 (TRPC6). *J. Biol. Chem.* **293,** 10381–10391 CrossRef Medline
70. Tang, Q., Guo, W., Zheng, L., Wu, J. X., Liu, M., Zhou, X., Zhang, X., and Chen, L. (2018) Structure of the receptor-activated human TRPC6 and TRPC3 ion channels. *Cell Res.* **28,** 746–755 CrossRef Medline
71. Chiluiza, D., Krishna, S., Schumacher, V. A., and Schlöndorff, J. (2013) Gain–of–function mutations in transient receptor potential C6 (TRPC6) activate extracellular signal-regulated kinases 1/2 (ERK1/2). *J. Biol. Chem.* **288,** 18407–18420 CrossRef Medline
72. Aviram, N., Ast, T., Costa, E. A., Arakel, E. C., Chuartzman, S. G., Jan, C. H., Hassdenteufel, S., Dudek, J., Jung, M., Schorr, S., Zimmermann, R., Schwappach, B., Weissman, J. S., and Schuldiner, M. (2016) The SND proteins constitute an alternative targeting route to the endoplasmic reticulum. *Nature* **540,** 134–138 CrossRef Medline
73. Yu, H., Kistler, A., Faridi, M. H., Meyer, J. O., Tryniszewska, B., Mehta, D., Yue, L., Dryer, S., and Reiser, J. (2016) Synaptopodin limits TRPC6 podocyte surface expression and attenuates proteinuria. *J. Am. Soc. Nephrol.* **27,** 3308–3319 CrossRef Medline
74. Doench, J. G., Fusi, N., Sullender, M., Hegde, M., Vaimberg, E. W., Donovan, K. F., Smith, I., Tothova, Z., Wilen, C., Orchard, R., Virgin, H. W., Listgarten, J., and Root, D. E. (2016) Optimized sgRNA design to maximize activity and minimize off-target effects of CRISPR-Cas9. *Nat. Biotechnol.* **34,** 184–191 CrossRef Medline
75. Ruggiano, A., Foresti, O., and Carvalho, P. (2014) Quality control: ER-associated degradation: protein quality control and beyond. *J. Cell Biol.* **204,** 869–879 CrossRef Medline
76. Olzmann, J. A., Kopito, R. R., and Christianson, J. C. (2013) The mammalian endoplasmic reticulum-associated degradation system. *Cold Spring Harb. Perspect. Biol.* **5,** a013185 CrossRef Medline
77. Dettmer, U., Kuhn, P. H., Abou-Ajram, C., Lichtenthaler, S. F., Krüger, M., Kremmer, E., Haass, C., and Haffner, C. (2010) Transmembrane protein 147 (TMEM147) is a novel component of the Nicalin–NOMO protein complex. *J. Biol. Chem.* **285,** 26174–26181 CrossRef Medline
78. Kumar, R., Yang, J., Larsen, R. D., and Stanley, P. (1990) Cloning and expression of *N*-acetylglucosaminyltransferase I, the medial Golgi transferase that initiates complex *N*-linked carbohydrate formation. *Proc. Natl. Acad. Sci. U.S.A.* **87,** 9948–9952 CrossRef Medline
79. Christianson, J. C., Olzmann, J. A., Shaler, T. A., Sowa, M. E., Bennett, E. J., Richter, C. M., Tyler, R. E., Greenblatt, E. J., Harper, J. W., and Kopito, R. R. (2011) Defining human ERAD networks through an integrative mapping strategy. *Nat. Cell Biol.* **14,** 93–105 CrossRef Medline
80. Guna, A., Volkmar, N., Christianson, J. C., and Hegde, R. S. (2018) The ER membrane protein complex is a transmembrane domain insertase. *Science* **359,** 470–473 CrossRef Medline
81. Satoh, T., Ohba, A., Liu, Z., Inagaki, T., and Satoh, A. K. (2015) dPob/EMC is essential for biosynthesis of rhodopsin and other multi-pass membrane proteins in *Drosophila* photoreceptors. *Elife* **4,** CrossRef Medline
82. Zhao, Y., Hu, J., Miao, G., Qu, L., Wang, Z., Li, G., Lv, P., Ma, D., and Chen, Y. (2013) Transmembrane protein 208: a novel ER-localized protein that regulates autophagy and ER stress. *PLoS One* **8,** e64228 CrossRef Medline
83. Dietrich, A., Mederos y Schnitzler, M., Emmel, J., Kalwa, H., Hofmann, T., and Gudermann, T. (2003) *N*-Linked protein glycosylation is a major determinant for basal TRPC3 and TRPC6 channel activity. *J. Biol. Chem.* **278,** 47842–47852 CrossRef Medline
84. Doleschal, B., Primessnig, U., Wolkart, G., Wolf, S., Schernthaner, M., Lichtenegger, M., Glasnov, T. N., Kappe, C. O., Mayer, B., Antoons, G., Heinzel, F., Poteser, M., and Groschner, K. (2015) TRPC3 contributes to regulation of cardiac contractility and arrhythmogenesis by dynamic interaction with NCX1. *Cardiovas. Res.* **106,** 163–173 CrossRef Medline
85. Xu, X., Lozinskaya, I., Costell, M., Lin, Z., Ball, J. A., Bernard, R., Behm, D. J., Marino, J. P., Jr., and Schnackenberg, C. G. (2013) Characterization of small molecule TRPC3 and TRPC6 agonist and antagonists. *Biophys. J.* **104,** 454
86. Ambudkar, I. S. (2007) Trafficking of TRP channels: determinants of channel function. *Handb. Exp. Pharmacol.* 541–557 CrossRef Medline
87. Greka, A., Navarro, B., Oancea, E., Duggan, A., and Clapham, D. E. (2003) TRPC5 is a regulator of hippocampal neurite length and growth cone morphology. *Nat. Neurosci.* **6,** 837–845 CrossRef Medline
88. Bezzerides, V. J., Ramsey, I. S., Kotecha, S., Greka, A., and Clapham, D. E. (2004) Rapid vesicular translocation and insertion of TRP channels. *Nat. Cell Biol.* **6,** 709–720 CrossRef Medline
89. Xie, J., Cha, S. K., An, S. W., Kuro-O, M., Birnbaumer, L., and Huang, C. L. (2012) Cardioprotection by Klotho through downregulation of TRPC6 channels in the mouse heart. *Nat. Commun.* **3,** 1238 CrossRef Medline
90. Chaudhuri, P., Rosenbaum, M. A., Sinharoy, P., Damron, D. S., Birnbaumer, L., and Graham, L. M. (2016) Membrane translocation of TRPC6 channels and endothelial migration are regulated by calmodulin and PI3 kinase activation. *Proc. Natl. Acad. Sci. U.S.A.* **113,** 2110–2115 CrossRef Medline
91. de Souza, L. B., and Ambudkar, I. S. (2014) Trafficking mechanisms and regulation of TRPC channels. *Cell Calcium* **56,** 43–50 CrossRef Medline
92. Krall, P., Canales, C. P., Kairath, P., Carmona-Mora, P., Molina, J., Carpio, J. D., Ruiz, P., Mezzano, S. A., Li, J., Wei, C., Reiser, J., Young, J. I., and Walz, K. (2010) Podocyte-specific overexpression of wildtype or mutant trpc6 in mice is sufficient to cause glomerular disease. *PLoS One* **5,** e12859 CrossRef Medline

93. Saleem, M. A., O'Hare, M. J., Reiser, J., Coward, R. J., Inward, C. D., Farren, T., Xing, C. Y., Ni, L., Mathieson, P. W., and Mundel, P. (2002) A conditionally immortalized human podocyte cell line demonstrating nephrin and podocin expression. *J. Am. Soc. Nephrol.* **13,** 630–638 Medline
94. Wideman, J. G. (2015) The ubiquitous and ancient ER membrane protein complex (EMC): tether or not? *F1000Res.* **4,** 624 CrossRef Medline
95. Shurtleff, M. J., Itzhak, D. N., Hussmann, J. A., Schirle Oakdale, N. T., Costa, E. A., Jonikas, M., Weibezahn, J., Popova, K. D., Jan, C. H., Sinitcyn, P., Vembar, S. S., Hernandez, H., Cox, J., Burlingame, A. L., Brodsky, J. L., *et al.* (2018) The ER membrane protein complex interacts cotranslationally to enable biogenesis of multipass membrane proteins. *Elife* **7,** e37018 CrossRef Medline
96. Chitwood, P. J., Juszkiewicz, S., Guna, A., Shao, S., and Hegde, R. S. (2018) EMC is required to initiate accurate membrane protein topogenesis. *Cell* **175,** 1507–1519.e16 CrossRef Medline
97. Richard, M., Boulin, T., Robert, V. J., Richmond, J. E., and Bessereau, J. L. (2013) Biosynthesis of ionotropic acetylcholine receptors requires the evolutionarily conserved ER membrane complex. *Proc. Natl. Acad. Sci. U.S.A.* **110,** E1055–E1063 CrossRef Medline
98. Louie, R. J., Guo, J., Rodgers, J. W., White, R., Shah, N., Pagant, S., Kim, P., Livstone, M., Dolinski, K., McKinney, B. A., Hong, J., Sorscher, E. J., Bryan, J., Miller, E. A., and Hartman, J. L., 4th. (2012) A yeast phenomic model for the gene interaction network modulating CFTR-ΔF508 protein biogenesis. *Genome Med.* **4,** 103 CrossRef Medline
99. Casson, J., McKenna, M., Hassdenteufel, S., Aviram, N., Zimmerman, R., and High, S. (2017) Multiple pathways facilitate the biogenesis of mammalian tail-anchored proteins. *J. Cell Sci.* **130,** 3851–3861 CrossRef Medline
100. Hassdenteufel, S., Sicking, M., Schorr, S., Aviram, N., Fecher-Trost, C., Schuldiner, M., Jung, M., Zimmermann, R., and Lang, S. (2017) hSnd2 protein represents an alternative targeting factor to the endoplasmic reticulum in human cells. *FEBS Lett.* **591,** 3211–3224 CrossRef Medline
101. Usenovic, M., Knight, A. L., Ray, A., Wong, V., Brown, K. R., Caldwell, G. A., Caldwell, K. A., Stagljar, I., and Krainc, D. (2012) Identification of novel ATP13A2 interactors and their role in α-synuclein misfolding and toxicity. *Hum. Mol. Genet.* **21,** 3785–3794 CrossRef Medline
102. Przybylla, S., Stindt, J., Kleinschrodt, D., Schulte Am Esch, J., Häussinger, D., Keitel, V., Smits, S. H., and Schmitt, L. (2016) Analysis of the bile salt export pump (ABCB11) interactome employing complementary approaches. *PLoS One* **11,** e0159778 CrossRef Medline
103. Maddirevula, S., Alhebbi, H., Alqahtani, A., Algoufi, T., Alsaif, H. S., Ibrahim, N., Abdulwahab, F., Barr, M., Alzaidan, H., Almehaideb, A., AlSasi, O., Alhashem, A., Hussaini, H. A., Wali, S., and Alkuraya, F. S. (2019) Identification of novel loci for pediatric cholestatic liver disease defined by KIF12, PPM1F, USP53, LSR, and WDR83OS pathogenic variants. *Genet. Med.* **21,** 1164–1172 CrossRef Medline
104. Schneider, M., Al-Shareffi, E., and Haltiwanger, R. S. (2017) Biological functions of fucose in mammals. *Glycobiology* **27,** 601–618 CrossRef Medline
105. Zhivotovsky, B., and Orrenius, S. (2011) Calcium and cell death mechanisms: a perspective from the cell death community. *Cell Calcium* **50,** 211–221 CrossRef Medline
106. Thorburn, A. (2004) Death receptor-induced cell killing. *Cell. Signal.* **16,** 139–144 CrossRef Medline
107. Sanjana, N. E., Shalem, O., and Zhang, F. (2014) Improved vectors and genome-wide libraries for CRISPR screening. *Nat. Methods* **11,** 783–784 CrossRef Medline
108. Barger, C. J., Branick, C., Chee, L., and Karpf, A. R. (2019) Pan-cancer analyses reveal genomic features of FOXM1 overexpression in cancer. *Cancers* **11,** E251 CrossRef Medline
109. Stewart, S. A., Dykxhoorn, D. M., Palliser, D., Mizuno, H., Yu, E. Y., An, D. S., Sabatini, D. M., Chen, I. S., Hahn, W. C., Sharp, P. A., Weinberg, R. A., and Novina, C. D. (2003) Lentivirus-delivered stable gene silencing by RNAi in primary cells. *RNA* **9,** 493–501 CrossRef Medline
110. Yang, X., Boehm, J. S., Salehi-Ashtiani, K., Hao, T., Shen, Y., Lubonja, R., Thomas, S. R., Alkan, O., Bhimdi, T., Green, T. M., Johannessen, C. M., Silver, S. J., Nguyen, C., Murray, R. R., Hieronymus, H., *et al.* (2011) A public genome-scale lentiviral expression library of human ORFs. *Nat. Methods* **8,** 659–661 CrossRef Medline
111. Thakur, D. P., Tian, J. B., Jeon, J., Xiong, J., Huang, Y., Flockerzi, V., and Zhu, M. X. (2016) Critical roles of Gi/o proteins and phospholipase C-δ1 in the activation of receptor-operated TRPC4 channels. *Proc. Natl. Acad. Sci. U.S.A.* **113,** 1092–1097 CrossRef Medline